EFFECT OF SILICON CARBIDE (SIC) AND TUNGSTEN CARBIDE (WC) REINFORCEMENTS ON THE PROPERTIES OF (α)-SIALON CERAMIC-BASED NANO COMPOSITES

BY

RAJA MUHAMMAD AWAIS KHAN

A Thesis Presented to the

DEANSHIP OF GRADUATE STUDIES

KING FAHD UNIVERSITY OF PETROLEUM & MINERALS

DHAHRAN, SAUDI ARABIA

In Partial Fulfillment of the
Requirements for the Degree of

MASTER OF SCIENCE

In

MECHANICAL ENGINEERING

DECEMBER 2015

KING FAHD UNIVERSITY OF PETROLEUM & MINERALS

DHAHRAN- 31261, SAUDI ARABIA

DEANSHIP OF GRADUATE STUDIES

This thesis, written by **RAJA MUHAMMAD AWAIS KHAN** under the direction of his thesis advisor and approved by his thesis committee, has been presented and accepted by the Dean of Graduate Studies, in partial fulfillment of the requirements for the degree of **MASTER OF SCIENCE IN MECHANICAL ENGINEERING.**

Dr. Zuhar Gasem
Department Chairman

Dr. Tahar Laoui
(Advisor)

Dr. Salam A. Zummo
Dean of Graduate Studies

Dr.Abbas S. Hakeem
(Member)

22/3/16
Date

Dr. Saheb Nouari
(Member)

Dedicated to my beloved parents, sisters, brothers

&

my sincere wife

ACKNOWLEDGMENTS

All praise and many thanks are due to Allah, the Almighty, Who created the universe and sustains it; and Duruud and Salam be on the last of all the prophets (ﷺ) who made truth prevail over falsehood and provided humanity with guidance for all times.

My sincerest gratitude to King Fahad University of Petroleum and Minerals (KFUPM), Dhahran, Saudi Arabia for providing support and facilities to successfully accomplish this work. In addition to this, I would sincerely like to acknowledge Center of Research Excellence in Nanotechnology (CENT), in the Research Institute, along with its team, for the exceptional knowledge and expertise that I gained during my tenure.

I would like to express my deepest appreciation to my thesis advisor Dr. Tahar Laoui for his moral support and sincere advices; he continually and persuasively conveyed a spirit of adventure in regard to research. In addition to my advisor, I am also grateful to my thesis committee members, Dr. Abbas Saeed Hakeem and Dr. Nouari Saheb for their valuable contributions, guidance, support and encouragement throughout my research work.

I would also like to express my deepest gratitude to the faculty members of the Mechanical Engineering Department at KFUPM. Moreover, I am deeply indebted to Mr. Abdullatif Hashmi, Mr. Sadaqat and Mr. Idris for their support and cooperation in the experimental work.

I would also like to express my sincere appreciation to my colleagues in the Mechanical Engineering Department, especially Mr. Moath Mohammad Al Malki for helping me in different aspects of the thesis' work. Additionally, I would like to acknowledge my friends Azhar Ali Khan, Baqir Muhammad, Bilal Ahmed, Haider Tufail, Khwaja Muhammad, Khurram Shehzad, Muhammad Luqman, Muhammad Umer Khan, Muhammad Usman, Umais Khan, Umer Qayyum Sair, Waleed Umer and Wasem Razzaq. Without their help, it would have been impossible for me to finish my M.S. study.

Last, But not the least, I would like to thank my parents for their endless love and support; who, although far away from me, were always close to my thoughts and heart. I would also like to thank my wife, sisters and brothers for their moral support and encouragement.

TABLE OF CONTENTS

LIST OF TABLES

LIST OF FIGURES

LIST OF ABBREVIATIONS

α	Alpha
β	Beta
SiC	Silicon Carbide
SiC (μm)	Silicon Carbide (micro meter)
SiC (nm)	Silicon Carbide (nano meter)
WC (μm)	Tungsten Carbide (micro meter)
SPS	Spark Plasma Sintering
HIP	Hot-Isostatic Press
HP	Hot Press
GPS	Gas Pressure Sintering
PLS	Pressure-less Sintering
SEM	Scanning Electron Microscopy
BSE	Back Scattered Electron
EDS	Energy Dispersive Spectroscopy
nm	Nanometer
μm	Micrometer
Hv	Vickers Hardness
hr	Hour
Min	Minutes
MPa	Mega pascal
GPa	Giga Pascal
wt. %	Weight Percent

ABSTRACT

Full Name : Raja Muhammad Awais Khan

Thesis Title : Effect of Silicon Carbide (SiC) and Tungsten Carbide (WC) Reinforcements on the Properties of (α)-SIALON Ceramic-Based Nano Composites

Major Field : Mechanical Engineering

Date of Degree : December, 2015

SiAlON-based ceramics have been widely used as high temperature materials due their superior mechanical and thermal properties. These ceramics exhibit excellent combination of high strength, hardness, wear resistance and are chemically stable even at elevated temperature. As a result, SiAlON based ceramics possess great potential for applications where high wear resistance, thermal stability and strength are required.

In the present study, α-SiAlON, one of the major phases of SiAlON ceramics, was used as a matrix for producing composites. Dense single phase (monolithic) α-SiAlON exhibiting high mechanical properties, namely hardness (Hv_{10} 21.06 GPa) and fracture toughness (7.29 $MPa.m^{1/2}$), was synthesized by using nano-sized powder precursors and calcium oxide (CaO) as an additive, via spark plasma sintering technique (SPS) for consolidation at a relatively low temperature of 1500 °C and holding time of 30 min.

Micron sized silicon carbide SiC (~ 2 μm) particles, up to 30 weight % (wt. %), were successfully dispersed as a second phase in the α-SiAlON matrix to further enhance the mechanical properties of the composite ceramics. For α-SiAlON composites reinforced with SiC (μm), the highest hardness of 24.53 GPa (Hv_{10}) and highest fracture toughness of 11.86 $MPa.m^{1/2}$ were achieved for 30 wt. % SiC (μm).

Sialon composites prepared with nano-size silicon carbide SiC (50 nm) did not yield good results due to poor dispersion and formation of SiC clusters within the matrix.

Composite ceramic with micron sized tungsten carbide WC (~ 3.5 μm) showed homogenous dispersion for composite with 10 weight % WC, while the level of dispersion decreased with increase in amount of second phase. For α-SiAlON/10 wt. % WC (μm) composite, the hardness and fracture toughness were measured to be 23.46 GPa (Hv_{10}) and 19.42 MPa.$m^{1/2}$ respectively.

ملخص الرسالة

الاسم الكامل: راجا محمد اوس خان

عنوان الرسالة: تأثير كل من كربيد السيلكون و كربيد التنغستون على تقوية خصائص سيرميكيات النانو ال α -SIALON

التخصص: الهندسة الميكانيكية

تاريخ الدرجة العلمية: ديسمبر, 2015

عرفت مواد السايلون السيراميكية كمواد ملائمة لدرجات الحرارة العالية بسبب خواصها الحرارية والميكانيكية المتميزة، كالقوة والصلابة و مقاومة التآكل والاستقرار الكيميائي في درجات الحرارة العالية، وهو ما يجعلها مناسبة للتطبيقات التي تتطلب مقاومة التآكل والاستقرار الحراري والقوة.

في هذه الدراسة، استخدم طور الألفا-سايلون كمادة الأساس لتطوير المادة المركبة. استخدمت المواد الأولية في حجم النانو إلى جانب إضافة أكسيد الكالسيوم لتحضير طور الألفا –سايلون منفردا في صورة عالية الكثافة ، والذي انعكس على خواص ميكانيكية عالية ممثلة في الصلابة (21.06 GPa) والمتانة ($7.29\ MPa.m^{1/2}$). حضر طور الألفا-سايلون بتقنية التلبيد بالشرارة الكهربائية والبلازما على درجة حرارة منخفضة نسبيا (1500 °C) و في وقت قصير نسبيا (30 دقيقة).

خلطت جسيمات كاربيد السيليكون المايكرونية ($\approx 2\ \mu m$) بشكل ناجح مع طور الألفا-سايلون، والمضافة بوزن يصل حتى 30% من وزن الألفا سايلون لتطوير الخصائص الميكانيكية للمادة المركبة. بلغت أعلى قيمة للصلابة لمركب الألفا-سايلون وجسيمات كاربيد السيليكون المايكرونية -بوزن قدره 30% من وزن الأول- 24.53 GPa، بينما بلغت أعلى قيمة للمتانة $11.86\ MPa.m^{1/2}$.

مركب الألفا-سايلون و جسيمات كاربيد السيليكون النانوية (50 nm) لم يظهر خواصا ميكانيكية جيدة بسبب ضعف توزع الجسيمات في مادة الأساس (الألفا-سايلون).

أظهرت جسيمات كاربيد التنجستن المايكرونية ($3.5\ \mu m$) توزعا متجانسا في مركبها مع الألفا-سايلون إذا كان وزن الجسيمات 10% من وزن مادة الأساس (الألفا-سايلون)، بينما يبتدهور هذا التوزع كلما زادت كمية الجسيمات المضافة. أظهرت القياسات أن خاصية الصلابة لمركب الألفا-سايلون و كاربيد التنجستن (10%) تساوي، 23.46 GPa بينما كانت قيمة المتانة $19.42\ MPa.m^{1/2}$.

CHAPTER 1

INTRODUCTION

Si_3N_4 ceramics have been shown to sustain severe working conditions due to their remarkable mechanical and thermal properties, namely hot hardness, chemical inertness and thermal shock resistance [1]. However, full densification of Si_3N_4 powder compacts using conventional solid-state sintering technique has proven difficult without applying excess pressure and temperature. This is attributed to the covalent bonding present between Si and N atoms that inhibits any lattice diffusion from taking place as atomic species become sufficiently mobile for densification at temperatures >1850°C where decomposition of silicon nitride commences [2, 3]. Thus, alternative approaches are necessary involving mixing metal oxide additives with silicon nitride powder to provide appropriate conditions for liquid phase sintering [1, 2, 3] .The types and amounts of additives used for sintering determine the nature and quantity of the resulting grain boundary phase and hence the mechanical properties. The use of alumina combined with other oxides as sintering additives has been a significant milestone in the development of SiAlON ceramics [4, 5, 6].

SiAlONs are solid solutions of α-silicon nitride and β-silicon nitride, in which part of the Si and N is replaced by Al and O, respectively, in a simultaneous process to maintain charge neutrality [4, 6]. In particular, α- and β- SiAlONs have attracted much attention in the past

two decades due to their exceptional mechanical properties, namely high hardness for α-SiAlON and reasonable fracture toughness for β-SiAlON [7, 8].

α-SiAlONs are based on the α-$Si_{12}N_{16}$ unit cell with stoichiometric formula [4]: $M_x Si_{12-(m+n)} Al_{(m+n)} O_n N_{16-n}$ where m is the number of Al-N bonds, n is the number of Al-O bonds, M represents the added cation such as many of the lanthanides, rare earth and alkaline earth elements, $x = m/v \leq 2$ where v indicates the valence of the added cation. α-SiAlON is formed from the reaction of silicon nitride, aluminum nitride, aluminum oxide and the oxide of an appropriate modifying cation M (Y_2O_3, CaO, etc.) and densification occurs by liquid phase sintering. α-SiAlON is precipitated during the reaction and the amount of liquid gradually reduces until, theoretically, complete formation of α solid solution occurs. In practice, large amount of oxide additives are required to facilitate the densification process, however, this usually results in large amount of the liquid phase [4, 9].

Generally, α-SiAlON possesses higher hardness than β–SiAlON, while the latter shows better fracture toughness than the former. The reason behind this variation in the mechanical properties is explained usually through the consideration of the phase morphologies, in which α-SiAlON is formed mainly as equiaxed grains, while β–SiAlON grains tend to form elongated hexagonal prisms. However, scientists have successfully developed ceramics with elongated α-SiAlON grains to enhance its fracture toughness [10, 11]. Both α and β-SiAlONs have a hexagonal closed pack (HCP) crystal structure and their stacking sequence is ABCD and ABAB respectively [12]. Figure 1 shows the

representative phase diagram for SiAlON ceramics schematically showing regions of α and β SiAlONs.

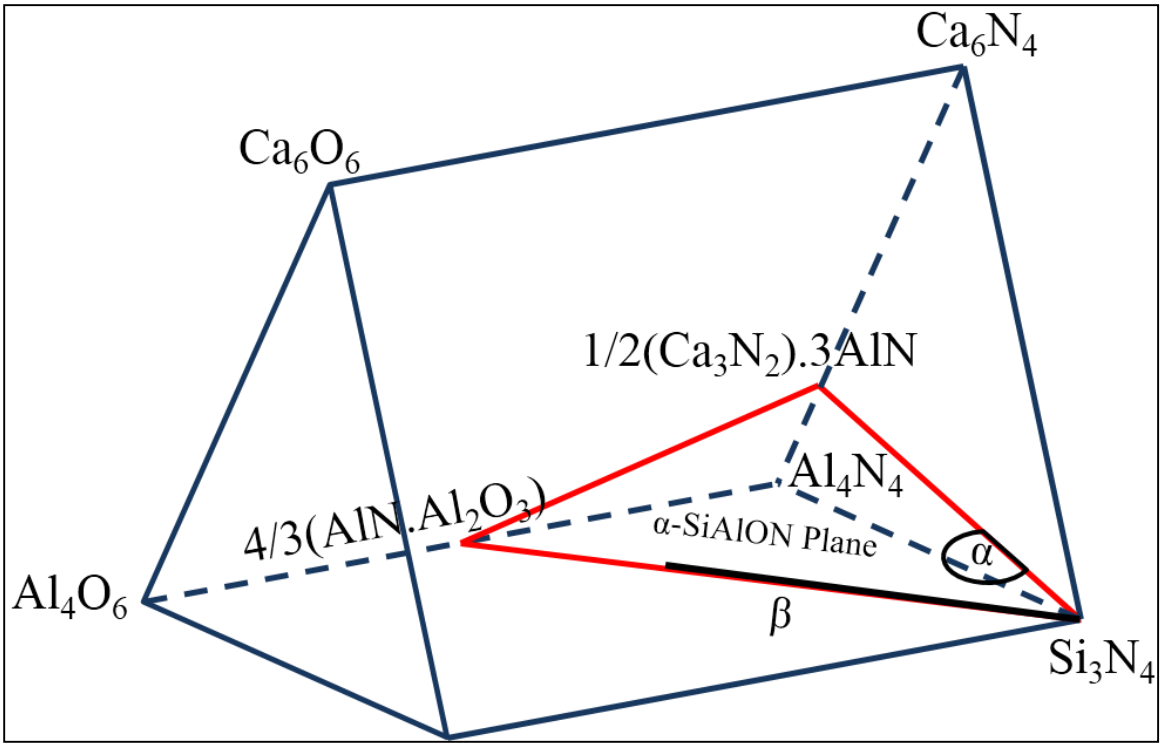

Figure 1: Janecke prism (Phase diagram of SiAlON) [12]

Rare earth sintering additives, such as oxides of Neodymium (Nd), Lanthanum (La), Yttrium (Y) and Ytterbium (Yb), have predominately been the major research interest in the last decade [13, 14, 15]. However, because of the relatively high cost in addition to crystal defects of these rare earths [16], the research focus has shifted to other additives, such as alkaline earth elements, namely Barium (Ba), Magnesium (Mg) and Calcium (Ca). Among the aforementioned elements, Ca seems to be the promising candidate to replace many of the lanthanide additives as it can be incorporated easily into the α-SiAlON structure without any notable crystal distortion [17, 18]. Further, it can be easily formed from fly ash, which explains the relative low price of Ca compounds compared with other alternatives [19].

Nevertheless, the research of mankind never ends here. In order to have even better properties, researchers have started synthesizing composite ceramics based on SiAlONs. Alumina (Al_2O_3), silicon carbide (SiC), zirconia (ZrO_2), titanium nitride (TiN), cubic boron nitride (cBN), titanium carbo Nitride (TiCN) and tungsten carbide (WC) have been used as reinforcements to SiAlON matrix to form composite ceramics [20, 21, 22, 23]. The reinforcements in the form of whiskers, filaments and particles have been tested to further improve mechanical, wear and electrical properties of monolithic SiAlONs.

Over the last few years, researchers have utilized spark plasma sintering (SPS) as a consolidation technique for various powder mixtures to form ceramics. Compared to other sintering techniques, due to the high heating rate and pulsed nature of the current, SPS has confirmed its benefits of rapidly densifying compacted powders at relatively low energy input [24, 25, 26].

The present work aims to the development of α-SiAlON ceramic based composites. For the synthesis of the matrix, a composition from α-SiAlON region, nearer to Si_3N_4 corner of the phase diagram (Figure 1), was selected to a form hard monolithic α-SiAlON ceramic at the expense of fracture toughness. Consolidation was carried out using SPS utilizing nano size starting powders. The compensation for the loss of fracture toughness was then addressed with the following reinforcements; silicon carbide (SiC) and tungsten carbide (WC), added to α-SiAlON matrix to produce high wear resistance composite ceramics.

The sintering parameters, namely temperature and holding time, for the fabrication of monolithic α-SiAlON were varied to achieve a single phase α-SiAlON. The microstructures and properties of the produced monolithic α-SiAlON and α-SiAlON based ceramic composites reinforced with silicon carbide (SiC) and tungsten carbide (WC) were investigated.

The development of SiAlON-based ceramic composites will have great impact in the field of cutting/drilling tool industry. It is highly desirable to cut-down the cost of the cutting tools by increasing its lifetime while, also directly associated with the cost of energy sector. Therefore, an improved tool life impacts both productivity and cost/energy.

CHAPTER 2

LITERATURE REVIEW

SiAlON as mentioned in previous chapter has two well-known phases which are of major concern for preparing hard ceramics. A handsome amount of literature have been published for fabrication of monolithic sialons (α, β and other phases) to get optimum or desired properties for particular applications by changing sintering/synthesizing techniques like gas pressure sintering, hot-pressing (HP), hot-isostatic pressing (HIP), pressure less sintering and spark plasma sintering (SPS) [25, 27, 28]. The study of variation in synthesis parameters like heating rate, sintering temperature and holding time on the mechanical, electrical, thermal, and shock resistance applications have been considered in abundance [29, 30, 31]. Several sialons compositions by changing the value of z in case of β-sialon, and 'm' and 'n' along with compensating cation in case of α-sialon have been studied with variety of precursors. The effect of sintering additives like rare earth and alkaline earth metal (oxides and carbonates) have also been studied by various research groups [14, 15, 32]. The effect of sintering additive from alkaline earth metal oxide has also got much attention for relaxing the sintering temperature for getting higher amount of α-phase in the end product. Although it's a known fact that α-sialon is harder as compared to β-sialon, and β-Sialon shows better fracture toughness values because of the elongated microstructure [33, 34, 27, 35, 36, 37].

Like most of the ceramics, second phase reinforcements are added to enhance the properties, sialons also got due consideration and some researches tried to inculcate

different types of hard particles and fibers reinforcements to form ceramics composites. A comprehensive literature review for silicon carbide and tungsten carbide reinforcements in sialons is represented in the remaining of this chapter.

2.1 Silicon Carbide Reinforced SiAlON Composites

The use of SiC as a reinforcement in Sialons is highlighted comprehensively in Table 1 and the same is explained in the coming paragraphs.

In 1990, Y. Akimune studied high-temperature strength of silicon carbide (SiC) whiskers sialon composites. Bending strength of specimens was tested at different elevated temperature. The specimen containing higher amount of SiC whiskers showed better strength at various temperatures as depicted in Figure 2. This increase in bending strength was associated to the inhibition of softening of glassy phase at the grain boundaries due to the presence of SiC whiskers which also resulted in the sustainability of composites to higher loads at elevated temperatures. These SiC whiskers at the grain boundaries, Figure 3, strengthen SiAlONs against intergranular fracture most prominently at high temperatures [38].

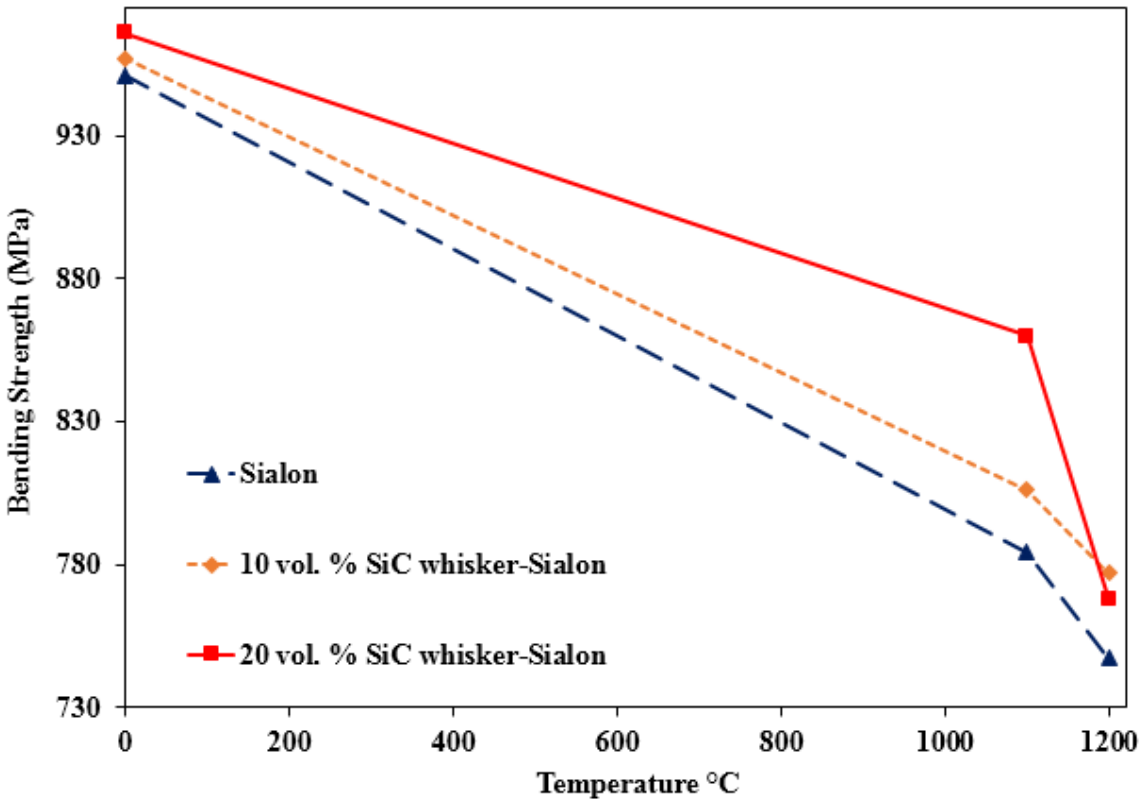

Figure 2: Bending strength as a function of temperature [38]

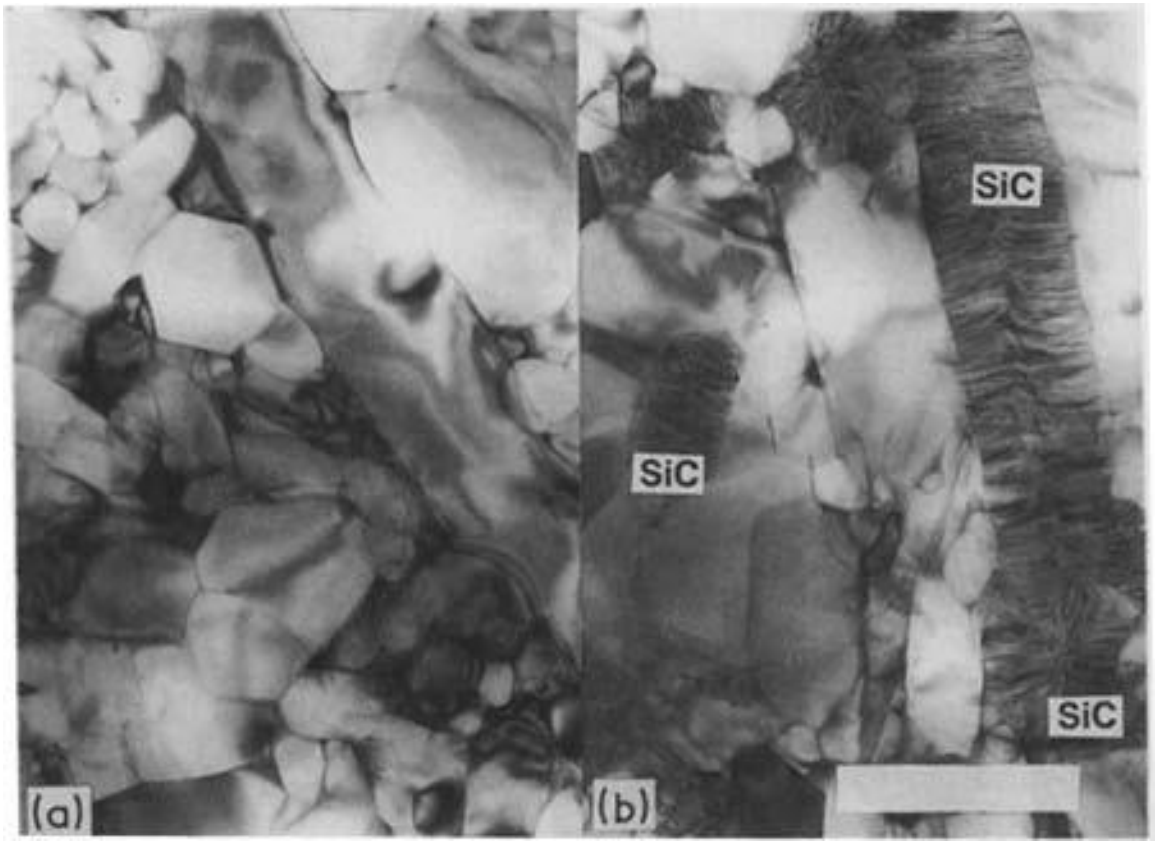

Figure 3: Transmission electron micrographs (bar is 10 nm). (a) Sialon and (b) 20 vol. % SiC whisker-Sialon [38]

Table 1: Literature for SiC reinforcements in SiAlONs

Author	Year	Matrix	Matrix Composition	Reinforcement	Mixing	Synthesis Technique	Hardness	Fracture Toughness
Y. Akimune	1990	Y-a-SiAlON	40 wt.% SiAlON & 60 wt.% Si_3N_4	(10-20 vol. %) β-SiC whiskers	Ball-Mill (ethanol, 24 h)	HP (1700 °C to 1840 °C, 30 min, 24.5 MPa, N_2)		Negligible affect: 5.2 MPa $m^{1/2}$, 5.3 MPa $m^{1/2}$(10 vol %), 5.2 MPa $m^{1/2}$(20 vol %)
Y. Akimune	1991	Y-a-SiAlON	40 wt.% SiAlON & 60 wt.% Si_3N_4	10 vol. % β-SiC particles (0.28 µm)	Ball-Mill (ethanol, 24 h)	HP(1720 °C, 30 min, 24.5 MPa, N_2), HIP (1850 °C & 1950 °C, 1h, 10 & 100 MPa, N_2 atmosphere)		4.6 MPa $m^{1/2}$(HP at 1720 °C), 5.6 MPa $m^{1/2}$(HIP at 1850 °C, 10 MPa N_2), 4.7 MPa $m^{1/2}$(HIP at 1850 °C, 100 MPa, N_2), 5.0 MPa $m^{1/2}$(HIP at 1950 °C, 100 MPa, N_2)
Chao. M Huang et al.	1994	β-SiAlON (80 % β-SiAlON & 20 % Al2O3)	$Si_{6-z}Al_z zO_zN_{8-z}$ z = 3	20 vol. % SiC monofilaments (140 µm dia, 2 inch length)	Uniaxially arranged in as-supplied SiAlON powder	HP (1600 °C, 2 h, 34 MPa, N_2)		Work of fracture (KJ m^{-2}): Increased from 2.67 to 16.7
Chao. M Huang et al.	1996	O-SiAlON	$Si_{2-x}Al_xN_{2-x}O_{1+x}$ x~0.14	20 vol. % SiC monofilaments (140 µm dia, 2 inch length)	Uniaxially arranged in as-supplied SiAlON powder	HP (1600 °C, 2 h, 34 MPa, N_2)		Work of fracture: Increased from 1.8 KJ m^{-2} to 42 KJ m^{-2}
H. Wang et al.	1997	Ca-a-SiAlON	$Ca_xSi_{12-(m+n)}Al_{m+n}O_nN_{16-n}$ x = 1, m = 2, n = 1	(0, 10, 20,30, 40 wt.%) SiC-(200 nm particles)	Milled (ethanol, 24 h)	HP (1700°C, 1 h, 25 MPa, 30°C/min)	HV_{10} (GPa) : 17.3, 17.7, 18.7, 18.8, 19 (From 0 to 40 wt.% SiC)	
Kazuo Ueno et al.	1997	β-SiAlON	$Si_{6-z}Al_zO_zN_{8-z}$, z = 3	(42 vol. % Carbon coated-filament # 500 & 48 vol. % uncoated-filament # 250) SiC fibre (Nicalon)	Slurry infiltration	HP (1350°C, 1 h, 20 MPa, N_2)		3.6 MPa $m^{1/2}$ (monolithic), 12.8 MPa $m^{1/2}$ (uncoated SiC composite)

Table 1: Literature for SiC reinforcements in SiAlONs (continued…)

Author	Year	Matrix	Matrix Composition	Reinforcement	Mixing	Synthesis Technique	Hardness	Fracture Toughness
Qiang Li et al.	1997	β-SiAlON		Nano-SiC powder (<60-70 nm), (10 wt. %)	Chemical technique	HP (1750°C, 1 h, 25 MPa)		
Q. Liu et al.	1999	α-SiAlON	$Ln_{m/3}Si_{12-(n+m)}Al_{m+n}O_nN_{16-n}$ (Ln = Nd, Dy, Yb, m=1, n=1.7)	Nano-SiC powder (30-60 nm), (10, 20 wt. %)	Chemical technique (PEG surfactant)	HP (1800 °C, 1 h, 30 MPa)	Figure 6	Figure 7
C. Santos et al.	2007	RE_2O_3 (Y_2O_3 45 wt.%, Yb_2O_3 19 wt.%, Er_2O_3 14wt.%, Dy_2O_3 11 wt. %)-α-SiAlON	80 vol.% Si_3N_4, 20 vol.% (AlN-RE_2O_3)	(0, 10, 15, 20 wt. %)-β-SiC	Planetary-Mill (Isopropilic alcohol, 2h)	GPS (1750 °C, 25 min/°C, 30min then 1950°C, 10 min/°C 1h, N_2) HP (1750 °C, 30mins, 20MPa)	Figure 8 (Hardness values at HV_2 (GPa)	Figure 9
Bernd Bitterlich et al.	2008	Mg-Y-(20-α & 80-β)-SiAlON		SiC (0.8 µm), WC (1.5 µm)-(10, 20, 30 vol.%)	Ball mill	Gas Pressure sintering (1930°C, 20bar N_2, 80bar Ar, 3 h)	HV_{10} (GPa)-max values: (without reinforcement 16), (25 vol. % SiC-20), (30 vol. % WC-18.8)	K_{IC} (MPa $m^{1/2}$)-max values: (without reinforcement 7), (15 vol. % SiC-6.6), (10 vol. % WC-6.1)
Limeng Liu et al.	2011	Y-α-SiAlON	$RE_{1/3}Si_{12-(m+n)}Al_{m+n}O_nN_{16-n}$ RE=Y, m=1, n=1 $Y_{1/3}Si_{10}Al_2ON_{15}$	(0, 5, 20, 40 wt. %)-SiC (powder)	Ball mill: Si_3N_4 balls, water free ethanol, 12 h	SPS (1800 °C, 5 min, 20 MPa, N_2, 100 °C/min)	HV_5 (GPa): 19.9, 20.7, 21.6, 22.8 (From 0 to 40 wt. % SiC)	K_{IC} (MPa $m^{1/2}$): 5.6, 7.3, 8.0, 8.2 (From 0 to 40 wt. % SiC)

In 1991, Y. Akimune et al. fabricated Sialon/SiC particulate composites. β-SiC particles were added into sialon to enhance its bending strength. The effect of varying sintering conditions was also studied. Highest strength was recorded for the specimen that was prepared by HIP at 1850°C under 100 MPa Nitrogen atmosphere. The increase in bending strength was attributed to the presence of β-SiC particles in the grain boundary which hindered the grain growth. Reduction in the grain size was also favored by the sintering parameters and conditions. The TEM micrographs showed spherically-shaped grains of α-sialon, needle like grains of β-sialon, and β-SiC particles (<0.1μm diameter) located in the glassy phase (grain boundaries) and within the grains. The effect of β-SiC addition on the fracture toughness of sialon was not discussed comprehensively. Although there was a negligible effect on the fracture toughness of the samples prepared using different sintering techniques and parameters with 10 vol. % addition of β-SiC [39].

Hot-Pressed β-SiAlON and O-SiAlON reinforced with silicon carbide (SiC) unidirectional monofilaments showed better fracture toughness and improved ultimate strength but lower resistance to first crack initiation as compared to monolithic β-SiAlON and O-SiAlON. The increase in work of fracture, i.e. fracture toughness, was attributed to filament pull-out, bridging and crack deflection among SiC filaments, as depicted in Figure 4. The tendency of filament-pullout during grinding resulted in relatively rough surface finish for composites as compared to monolithic β & O-SiAlONs, which in turns lowered the first crack initiation strength in the composites [40], [41].

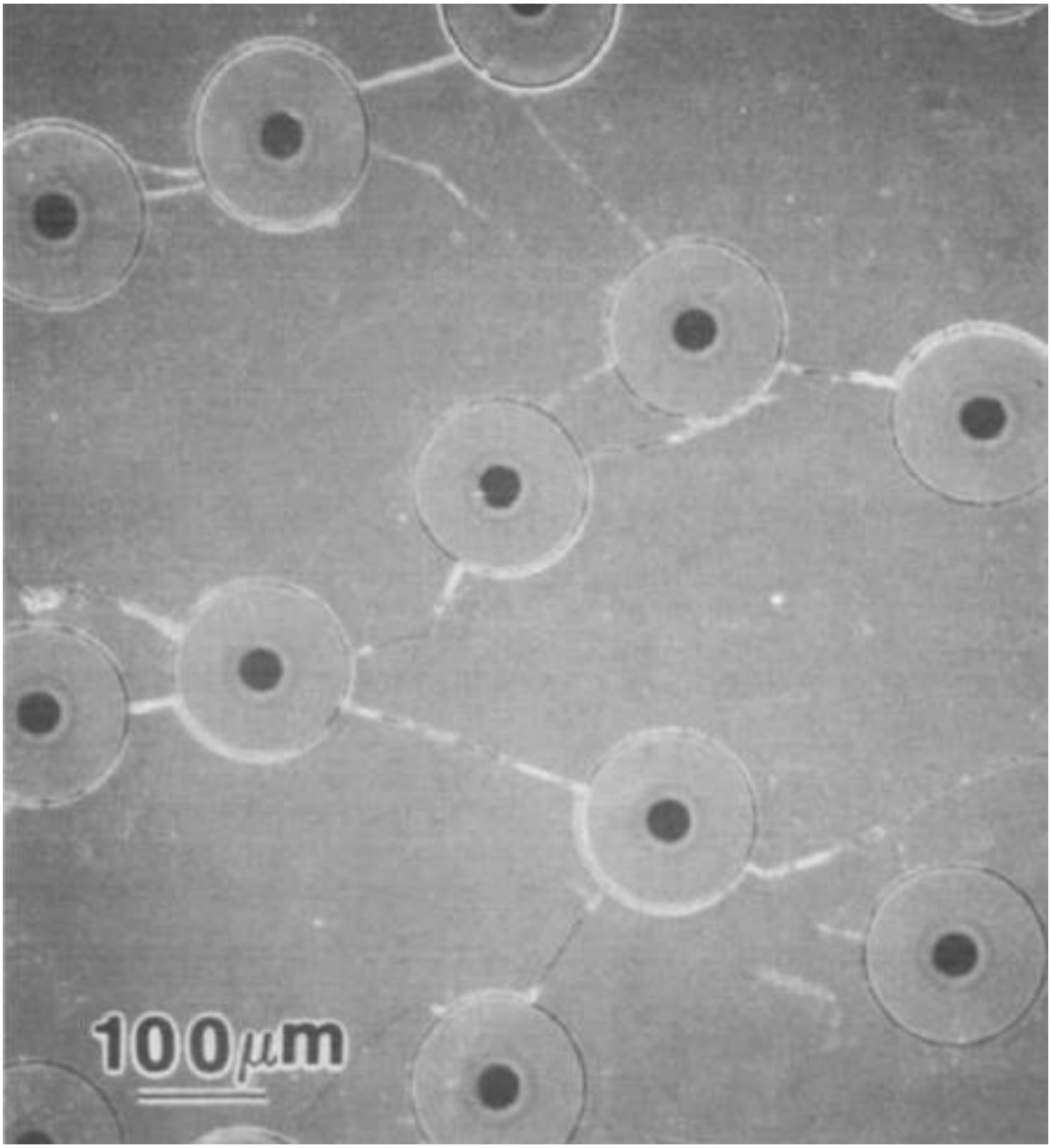

Figure 4: SEM of failed polished surface (crack propagation and deflection) [40]

Ca-α-SiAlON/β-SiC composites having nano-scale SiC (200 nm) particles prepared using hot pressing at temperatures of 1700 °C showed an increase in hardness with the increase in the amount of SiC from 0 wt. % to 40 wt. %. The uniformity in grain size distribution and refinement of grain size were attributed to the increase in hardness for samples with higher concentrations of SiC. Microstructural analysis depicted the presence of SiC particles at the grain boundaries which could have inhibited the grain growth and helped in refinement and uniformity of the grains. Moreover the sample containing 20 wt. % of SiC were sintered at temperatures of 1400 °C to 1800 °C with 100 °C increments to show the effectiveness of CaO as an additive for the densification of these ceramics by reducing the melting temperature of liquid phase. The relative amount of the phases present in the sintered specimens as a function of hot pressing temperature are shown in Figure 5. From the fact that sample (containing 20 wt. % of SiC) sintered at temperature of 1600 °C contained only α-SiAlON and SiC, one can easily recognized that the precipitation of α-phase and simultaneous densification of specimen at relatively lower temperature is the result of molten liquid phase provided by lower melting point of CaO [31]. But it should be noted that the use of nano size starting powders, because of their large surface areas and higher reactivity, could further reduce the melting temperature of the oxide phase with subsequent reduction in sintering temperature [42].

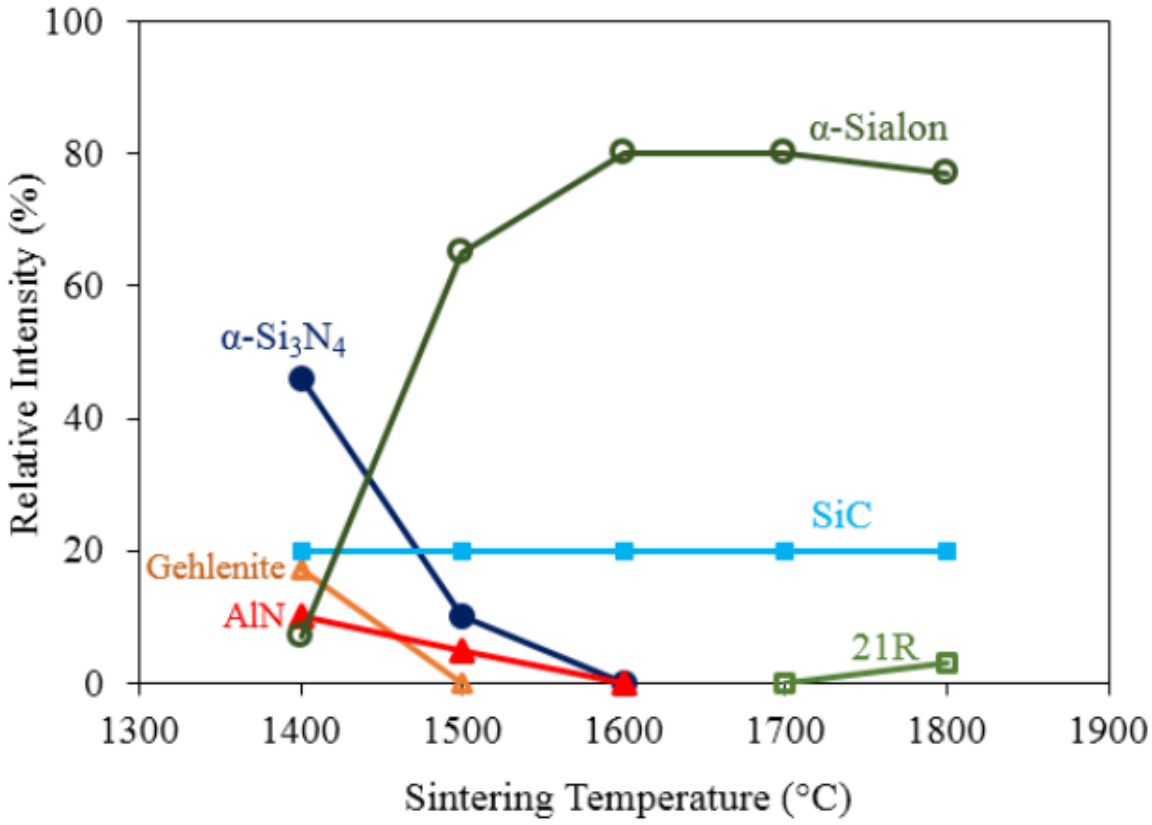

Figure 5: The relative fractions of the phases detected using x-ray diffraction of samples containing 20 wt. % SiC as function of hot-pressing temperature [31]

Kazuo Ueno et al., 1997, prepared SiC fibers (Nicalon) reinforced in β-Sialon powder using hot-press by incorporation of MgO-MgF_2 as a sintering additive. In order to reduce the thermal degradation of SiC fibers a lower sintering temperature was selected. The full relative densification of monolithic SiAlON suggested the effectiveness of these additives which promoted sintering at lower temperature by providing extra liquid phase. In order to make a comparison, these composites were fabricated using two types of SiC fibers; one coated with carbon and other without coating. The fracture toughness of composite obtained by non-coated fibers was found to be higher than monolithic β-SiAlON and it was explained by activation of fiber-bridging and/or fiber pull out mechanisms. In case of carbon coated Nicalon/SiAlON composite, delamination fracture was occurred probably due to the very weak interfacial bonding between the filaments and the matrix, because of which the fracture toughness was not calculated [43].

Chemical dispersion technique, polyacrylamide gel and surfactant, for mixing nano-sized SiC with starting powders (amounts in accordance with α-SiAlON phase) were used for preparing SiAlON/nano-SiC composite. Dy_2O_3 was used as a sintering aid in hot-pressing at temperature of 1750°C. It was shown that chemically treated sample helped to relax the sintering temperature as compared to un-treated sample due to homogeneous dispersion of nano-SiC particles. It was also shown that samples mixed using chemical mixing resulted in formation of pure β-SiAlON, despite the fact that the starting composition was selected in the pure α-SiAlON region. The sample prepared without chemical mixing technique sintered under the similar conditions showed formation of α-SiAlON. Therefore, it was postulated that probably nano-SiC and homogeneous mixing through chemical technique

not only helped to relax hot-pressing temperature but also resulted in the transformation of α-SiAlON to pure β-SiAlON. [44].

Q. Liu et al., used rare earth metal oxides as additives in single phase α-SiAlON as a starting composition along with reinforcements of different concentrations of SiC nano-powder. The thermal stability of α-phase in Neodymium Oxide (Nd_2O_3) samples was found to be much less than that of the samples sintered using Ytterbium Oxide (Yb_2O_3) and Dysprosium Oxide (Dy_2O_3) as additives. The enhanced transformation of α-Sialon to β-Sialon in Nd_2O_3 resulted in higher fracture toughness for these samples while the improved hardness for Yb- and Dy-stabilized samples was attributed to higher concentration of α-phase. It was also shown that the inculcation of SiC has very negligible effect on the amount of α-phase in the composite samples of all the three systems (Nd, Yb & Dy stabilized). The increase in hardness with increase in concentration of SiC (wt. %) was attributed to the addition of hard second phase. An important fact to be noted is the decrease in fracture toughness with increasing amount of SiC which was attributed to the lower aspect ratio of β-phase as compared to those present in monolithic samples. Moreover, SiC particles were observed to be present on the grain boundaries which also resulted in a comparatively circular morphology of β-grains leading to lower fracture toughness values. The hardness and fracture toughness of as-sintered Ln-Sialon/SiC composites as function of SiC concentration are shown in Figure 6 and Figure 7 respectively [45].

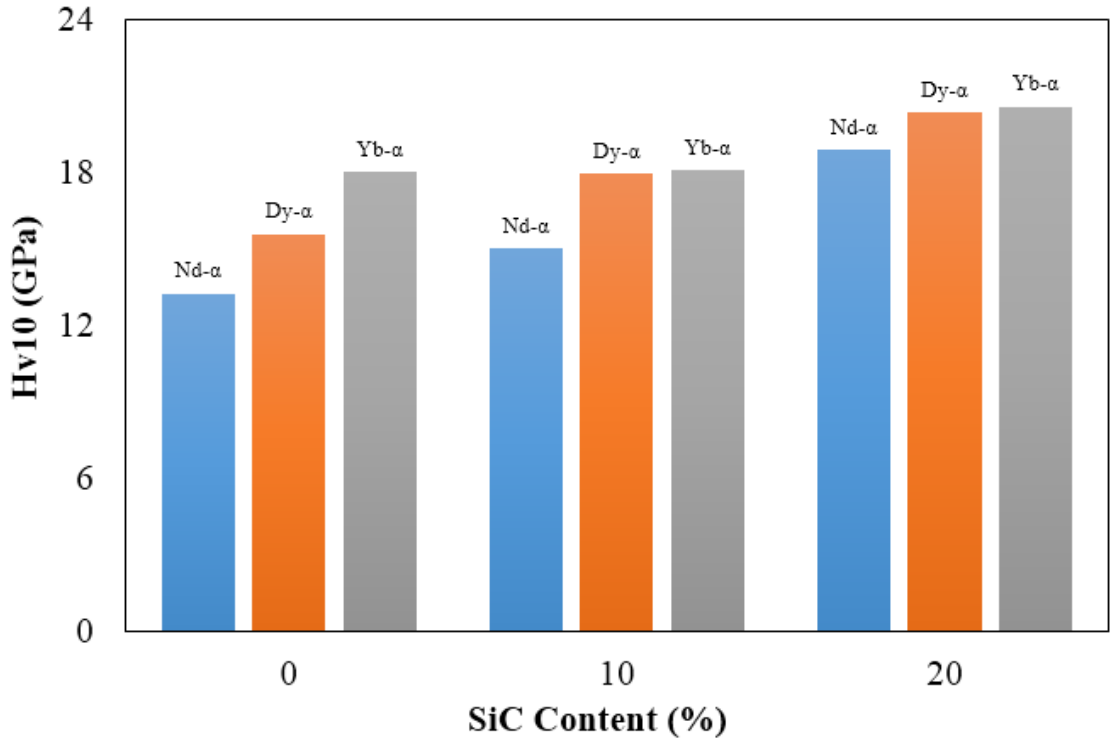

Figure 6: Vickers hardness vs. SiC additions in Ln-Sialon/SiC composites (Ln = Nd, Dy & Yb) [27]

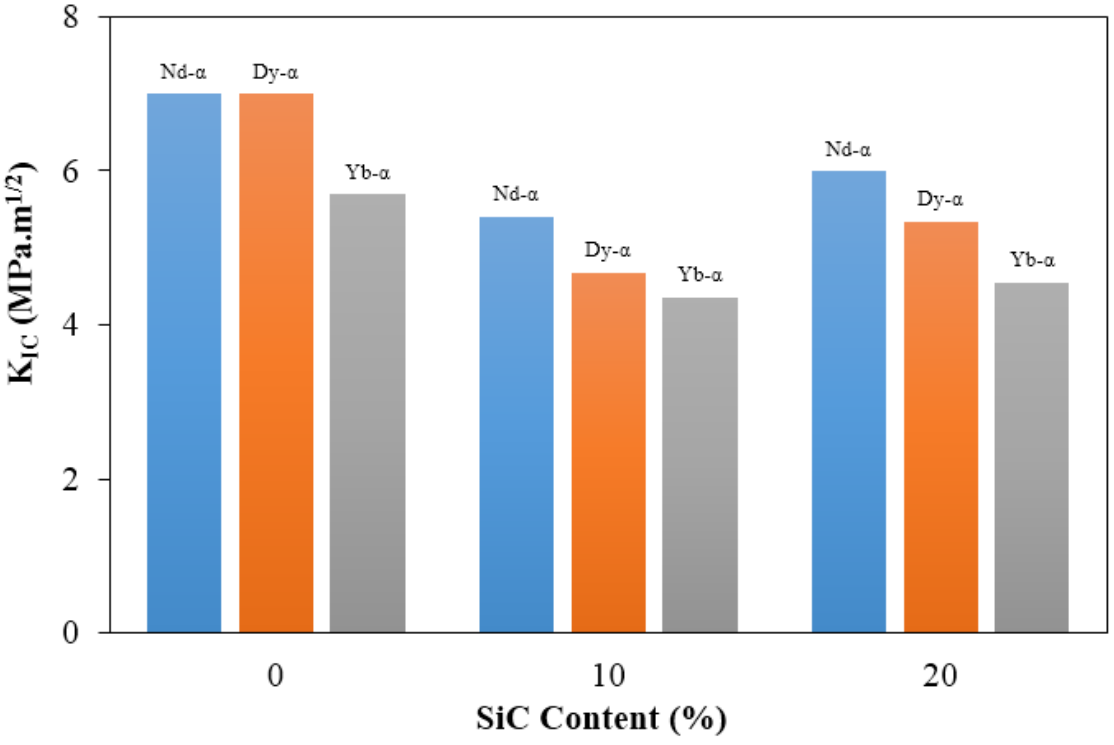

Figure 7: Fracture toughness vs. SiC additions in Ln-Sialon/SiC composites (Ln = Nd, Dy & Yb) [27]

In 2007, C. Santos showed the effect of adding different SiC concentrations by using two distinct synthesis techniques i.e. gas pressure sintering and hot-press for same α-SiAlON-SiC composites. Mixture of rare earth metal oxides was added as a sintering aid. Figure 8 and Figure 9 respectively show the hardness and fracture toughness results from the said source [46, 47]. The increase in hardness in hot pressed samples was attributed to higher hardness of SiC while the decrease in gas pressure sintered samples was due to poor densification of these samples in gas pressure sintering. Similarly, in the case of fracture toughness, with increase in SiC contents fracture toughness of samples prepared with both the techniques decreased which was associated to the inhibition of grain growth (with addition of SiC) resulting in lower grain size and a decreased aspect ratio which consequently resulted in lower fracture toughness of the composites [46, 47].

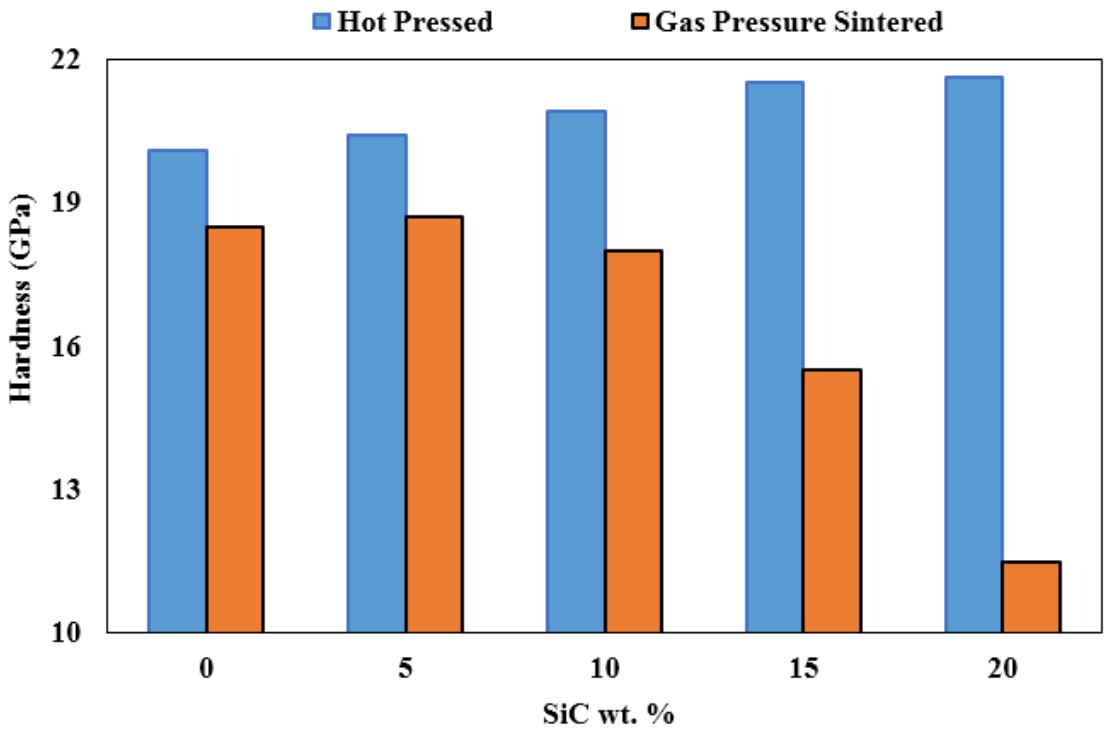

Figure 8: Influence of the SiC additions on hardness of α-SiAlON-SiC sintered samples [46, 47]

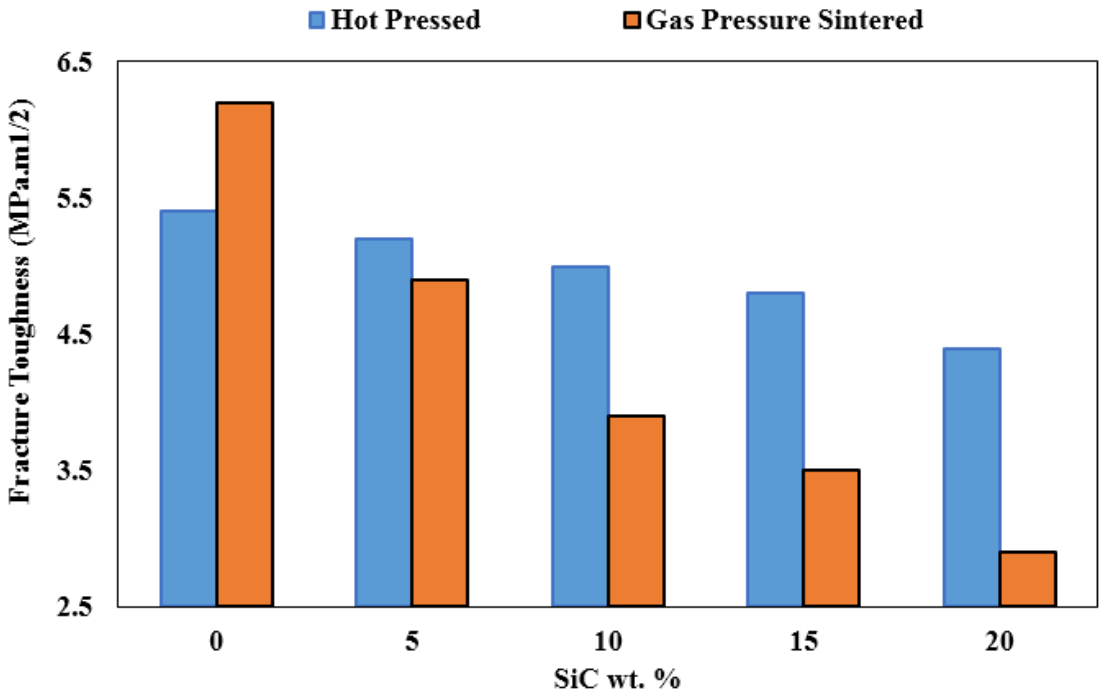

Figure 9: Influence of the SiC additions on fracture toughness of α-SiAlON-SiC sintered samples [46, 47]

α-SiAlON/α-SiC composites with varying concentrations of SiC (0 to 40 wt. %) were fabricated by Limeng Liu et al. using spark plasma sintering technique helped in growth of elongated grains. This elongated grain growth was attributed to presence of Y-SiAlON liquid phase and higher heating rates in spark plasma sintering. In this study it was highlighted that the anisotropic growth of SiC was not the β-cubic to α-hexagonal SiC (4H polymorph) phase transformation. Instead α-SiC (α-6H polymorph) phase remained the same as it was in the initial starting powder because of the thermodynamic stability of this phase below 2100 °C. Ostwald ripening was therefore correlated to this change in morphology from equiaxed to elongated grains which resulted in enhancement of fracture toughness. There was quite handsome increase in fracture toughness for specimens with 5 to 40 wt. % SiC due to larger crack deflection, friction pull out and deflection of cracks. Limeng Liu et al. also showed the increase in fracture toughness and flexural strength of these composites by heat treatment [26, 48].

2.2 Tungsten Carbide Reinforced SiAlON Composites

Tungsten carbide (WC) reinforcement in SiAlONs has not yet been considered in a true sense for enhancing the mechanical properties of SiAlONs. Very little amount of published resource was found for WC based SiAlON composites. The following paragraphs may be looked upon in this case although some information might be irrelevant as far as the scope of this research is concerned.

Erhan Ayas et al., 2004, studied the effect of WC addition in SiAlONs containing 50 % alpha and 50 % beta SiAlONs on the de-coloration of these ceramics prepared by gas pressure sintering [30].

Bernd Bitterlich et al., 2008, sintered SiAlON composites with 10, 20 & 30 vol. % of WC (0.8 μm particle size) in gas pressure sintering at 1930°C and studied the variation in hardness and fracture toughness with increase in WC contents, as depicted in Table 2. The starting matrix consisted of α/β ratio of 20:80 with magnesium and yttrium as sintering additives [49].

Table 2: Mechanical properties of WC-SiAlON composites [49]

WC (Vol. %)	HV_{10} (GPa)	K_{IC} ($MPa.m^{1/2}$)
0	16	7
10	18.5	6.1
20	18.8	5.9
30	17.2	5.8

The increase in the hardness and a decrease in fracture toughness with an increase in WC contents were attributed to increase in α/β phase ratio in the sintered samples. The sudden decrease in mechanical properties with 30 vol. % of WC was explained on the basis of porosity being found in the microstructure and also agglomeration of WC particles in the sample was seen although spray-drying have been used for drying the samples after mixing.

2.3 Aims and Objectives

The aim of the present study is to develop α-SiAlON based composite ceramics possessing high hardness and fracture toughness having potential wear resistance applications. This aim demands a deep understanding of such ceramics and composites, leading to the following objectives;

- To synthesis hard single phase monolithic α-SiAlON ceramics at lower temperatures utilizing nano scale starting powders.
- To synthesis dense α-SiAlON matrix by incorporation of Ca as a metal additive.
- To develop composite α-SiAlON based ceramics with reinforcement of SiC and WC.
- To utilize Spark Plasma Sintering (SPS) technique for developing monolithic and composite SiAlON ceramics in relatively short time and low temperature with less energy consumption and more economic process.
- To characterize the resultant microstructure, phase assemblage and physical/mechanical properties of the sintered SiAlONs.

CHAPTER 3

EXPERIMENTAL METHODOLOGY

3.1 Selection of α-SiAlON Composition

The first step in the experiment was to select a particular composition based on the general formula of α-SiAlONs by utilizing the phase diagram and the available literature. In order to achieve the objective of higher strength a composition near to Silicon Nitride corner of the phase diagram was selected. The general formula along with x, m and n values of the selected α-SiAlON composition are shown in Table 3. The x-value is calculated from the formula $x = {}^{m}/_{v}$, where v is the number of valences of the added cation i.e. Ca to the Si_3N_4 unit cell [50].

Table 3: SiAlON composition selected for the present study

No.	General Formula	X	m	N	Composition	N: O
1.	$\boldsymbol{Ca_x Si_{12-(m+n)} Al_{m+n} O_n N_{16-n}}$	0.8	1.6	1.2	$\boldsymbol{Ca_{0.8} Si_{9.2} Al_{2.8} O_{1.2} N_{14.8}}$	12:1

3.2 Powder Precursors

This section has been divided into two parts depending upon the role of the chemicals which were used during the course of this research. Firstly the powders which were present

in the matrix processing are mentioned. Later on the reinforcement which were inculcated in the matrix have been considered.

3.2.1 Starting Powders for the Matrix

The starting powder mixtures were prepared from alpha-Silicon Nitride (α-Si_3N_4) (150 nm-SN-10 Japan), Aluminum Nitride (AlN) (100 nm–Sigma-Aldrich, Germany), Silicon Oxide (SiO_2) (10-20 nm–Sigma-Aldrich, Germany) and Calcium Oxide (CaO) (<160 nm-Sigma-Aldrich, Germany). The details of all the starting precursors are shown in the Table 4.

Table 4: The starting powders and their sizes

Chemical	Company	Size (nm)
α-Si_3N_4	SN-10 Japan	150
AlN	Sigma Aldrich	100
Al_2O_3	Chempur	150
SiO_2	Sigma Aldrich	10-20
CaO	Sigma Aldrich	<160

3.2.2 Reinforcement Particles

Silicon Carbide micron-(SiC) (μm) (~ 2 μm, Buehler), Silicon Carbide nano-(SiC) (nm) (50 nm EPRUI Nanoparticles & Microspheres Co. Ltd) and Tungsten Carbide micron-(WC) (μm) (3.5 μm, William-Rowland Co., UK), were used as reinforcing particles in the α-SiAlON matrix. Figure 10 and Figure 11 show the scanning electron microscope images of micron sized and silicon carbide and tungsten carbide powders respectively. The average particle size of as received SiC-micron powder was 9.2 μm, which was higher than the

average particle size of WC-micron powder. Therefore in order to make a comparison between the two types of reinforcements, SiC was milled using high energy ball mill (Union Process HD01/HDDM) for 3 hours at 1000 revolution per minutes (RPM) using ethanol as a solvent. The estimated average particle size of SiC after ball milling was ~2 μm, which was determined by Microtrac-particles size analyzer (model S3500/Turbotrac). The particle size distribution for SiC (μm) after ball milling and for WC (μm) were determined by particle size analyzer using dynamic light scattering technique, as shown in Figure 12 and Figure 13 respectively.

Table 5 shows the names, size and company and/or condition of the reinforcement used in the present research. It should be noted that for sake of convenience micron sized Silicon Carbide, nano Silicon Carbide and Tungsten Carbide will be referred as SiC (μm), SiC (nm) and WC (μm) respectively in the rest of this report.

Table 5: Reinforcements

Reinforcement	Company	Size (μm) (as Received)	Milling Parameters	Size (μm) (after milling)
SiC (μm)	Buehler	9.2	HEBM (1000RPM- 3 hrs. -ethanol)	~ 2
WC (μm)	William-Rowland Co., UK	3.5	--	--
SiC (nm)	(EPRUI Nanoparticles & Microspheres Co. Ltd)	.05	--	--

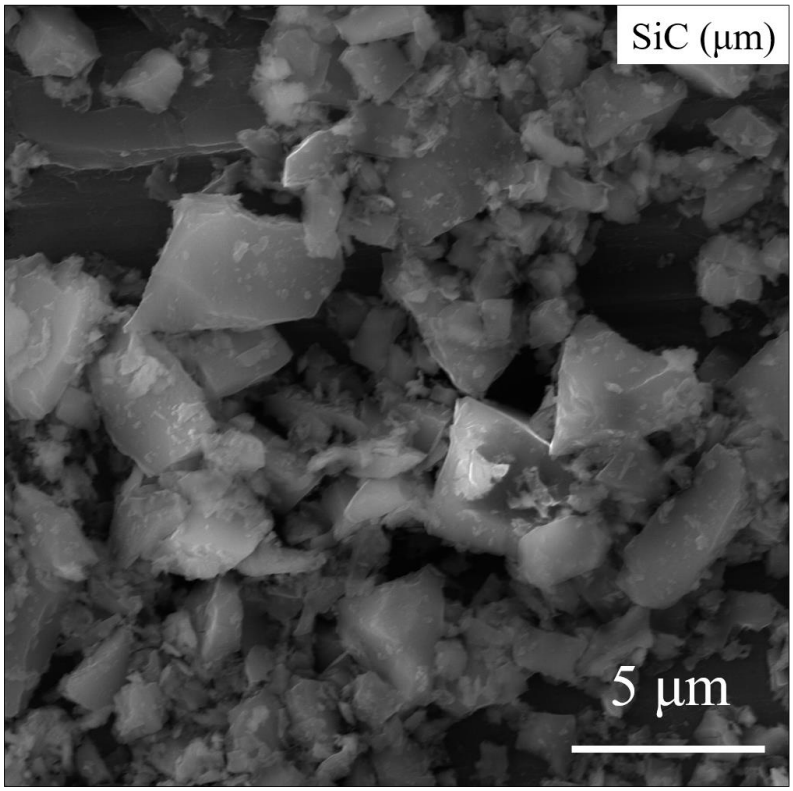

Figure 10: SEM of micron sized SiC after high energy ball milling, SiC (μm)

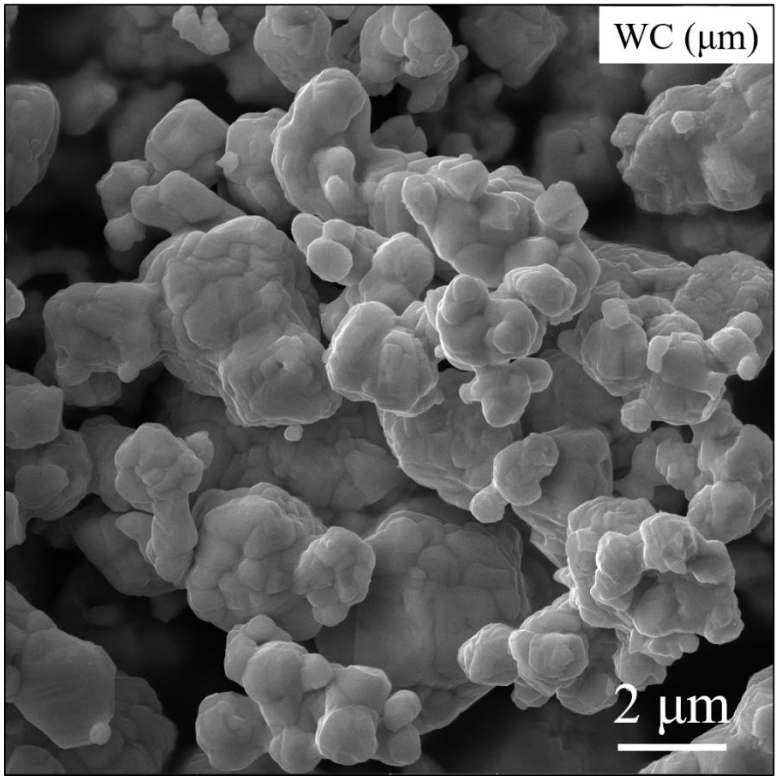

Figure 11: SEM of as received micron sized WC (μm)

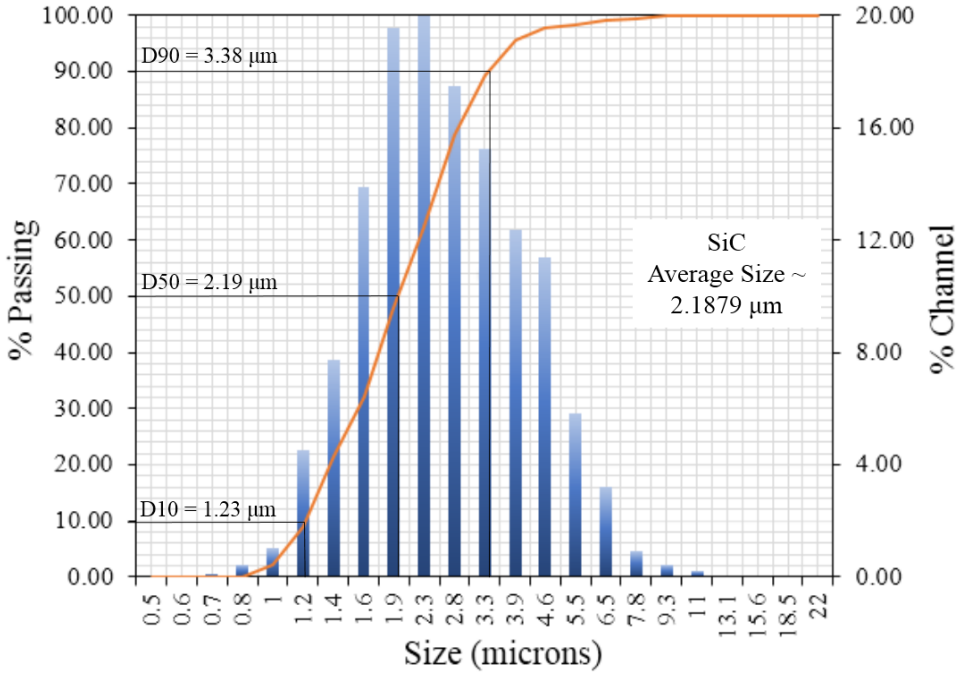

Figure 12: Particle size distribution of micron sized silicon carbide after ball milling SiC (µm)

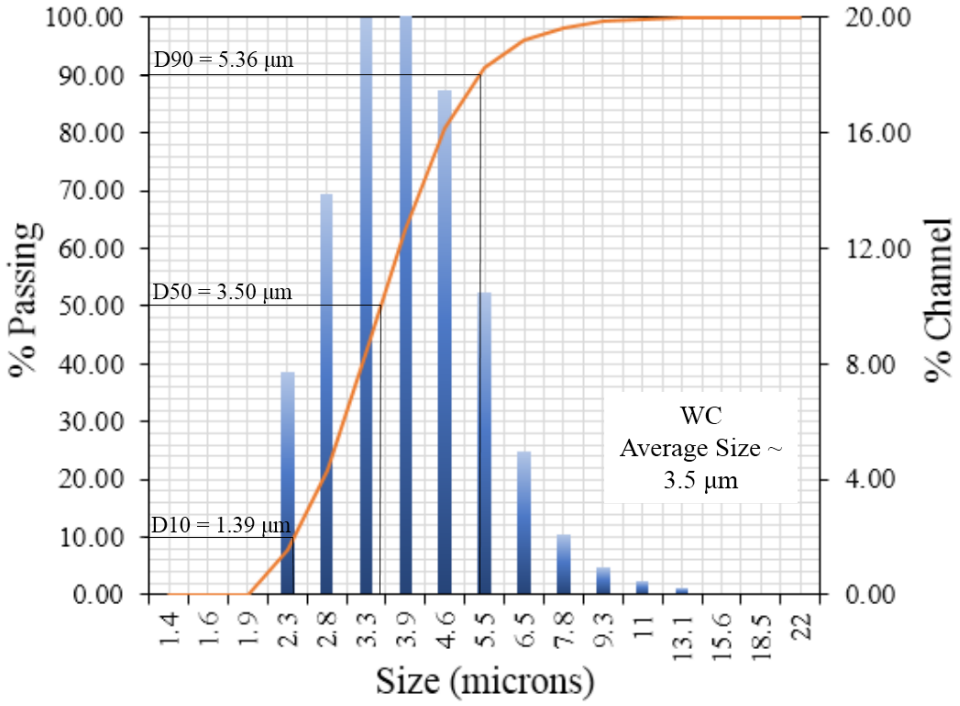

Figure 13: Particle size distribution of micron sized tungsten carbide WC (µm)

3.3 Mixing of Powders

Chemically balanced amount of the starting powders were carefully weighed before going for the mixing. For composite samples, (10, 20, 30) wt. % of the reinforcements were also added in the matrix powder. After carefully analyzing the effect of mixing time probe-sonication for 30 minutes in ethanol was selected as a mixing procedure. The mixing parameters were kept constant for all the samples (whether monolithic or composites). After mixing the solution was oven-dried at 80 °C to remove the solvent.

3.4 Consolidation of α-SiAlON Matrix

5 gram dried powder mixture prepared for each monolithic specimen was then poured into cylindrical graphite dies of 20 mm dia., after careful manual mixing in mortar and pestle to ensure homogeneity of the dried powder mixture. Graphite sheets were used on the inner walls of dies to eliminate direct contact of the powder with the dies. The poured powders were then sintered using spark plasma sintering (SPS) technique (Type HP D-50, FCT Systeme, Rauenstein, Germany) at two temperatures 1500 °C and 1600 °C with 10, 20 and 30 min holding time, at each temperature, under 50 MPa pressure at a heating rate of 100 °C/min with constant current and pulse duration. After holding at the sintering temperature for the specified time the samples were cooled quickly to room temperature.

3.5 Consolidation of α-SiAlON Based Composites

5 gram dried powder mixture prepared for each composite specimen, containing 10, 20 and 30 wt. % of reinforcements, was then poured into cylindrical graphite dies of 20 mm dia., after careful manual mixing in mortar and pestle to ensure homogeneity of the dried powder

mixture. Graphite sheets were used on the inner walls of dies to eliminate any direct contact of the powder with the dies. The poured powders were then sintered using spark plasma sintering (SPS) technique (Type HP D-50, FCT Systeme, Rauenstein, Germany) at a temperature of 1500 °C with 30 min holding time under 50 MPa pressure at a heating rate of 100 °C/min with constant current and pulse duration. After holding at the sintering temperature for the specified time the samples were cooled quickly to room temperature.

3.6 Characterization of Sintered Samples

3.6.1 Density Measurement

The sintered samples were cleaned, in order to remove any contamination from the graphite die and/or graphite sheets. Archimedes' principle was used to measure the density ρ of the cleaned specimens using the following equation:

$$\rho = \frac{A}{A - B}(\rho_0 - \rho_L) + \rho_L$$

$$\rho_L = 0.0012\ gm/cm^3\ ,\ \rho_0 = 1\ gm/cm^3$$

Where A indicates the sample weight in air and B indicates the sample weight in immersed liquid. The density of air is represented as ρ_0 while the density of the liquid in which the sample is immersed is represented as ρ_L.

Supposing that in composite samples the matrix is fully densified and have the same density as that of monolithic α-SiAlON sample [43] the theoretical densities of the composite samples have been calculated using the role of mixture in order to find the percentage densification of the samples. For which the density of the matrix was considered

the same as that obtained from the experimental density of monolithic α-SiAlON. While the densities of Silicon Carbide and Tungsten Carbide taken were 3.21 g/cm^3 and 15.6 g/cm^3 respectively.

3.6.2 Phase Analysis

After density measurements the cleaned samples were sliced in two half. One half was used for X-ray diffraction. X-ray diffraction (XRD) for phase identification was done using Rigaku MiniFlex X-ray diffractometer (Japan) with CuKα radiation (λ = 0.15416 nm) at 30 kV and 10 mA. The composition of the phases was determined and investigated by Rigaku data analysis software PDXL version 2.0.

3.6.3 Microstructural Analysis

The other half of the sliced samples was hot mounted in Buehler trans-optic powder (IL, USA) using IPA 40 Remet (Bologna, Italy). The mounted samples were then grinded using 74 μm, 40 μm, 20 μm and 9 μm diamond grinding pads, used particularly for hard materials and ceramics, in the mentioned sequence. The ground samples were then polished using diamond suspensions to 1/9 micron surface finish.

The fine polished specimens were then etched using different concentrations of hydrofluoric acid (HF) in order to reveal the microstructure. Field emission scanning electron microscope (FESEM, Lyra 3, Tescan, Czech Republic) was used to perform microstructural and fracture surface characterization at accelerating voltage of 30 kV in secondary and backscattered electron modes. The elemental composition of different phases was determined by energy dispersive X-ray (EDX) spectroscope (Oxford Inc., UK). The morphology of fracture surfaces was investigated in order to understand the fracture

behavior of the SiAlON ceramic composites. EDS Mapping was also done wherever needed, particularly for getting an idea of the dispersion level in composites.

3.6.4 Mechanical Properties

Universal hardness testing machine (Zwick-Roell, ZHU250, Germany) was used to measure Vickers hardness at 100 N load (Hv_{10}) using diamond pyramid indentor.

Fracture toughness testing shows wide variation in the field of hard materials. Single-Edge Notched Beam (SENB) and Single-edge V-Edge Notched Beam (SEVNB) are two leading techniques to evaluate fracture toughness, however none of these has been commercially standardized. One issue arises when applying these techniques is that samples should be relieved from residual stresses prior to testing [51]. Another limitation concerning our samples is the difficulty in initiating a pre-crack with the specified size. Further, the field of SiAlON has adopted unofficially the Indentation Method (IM). Hence, we got to stick to IM to offer a comparison sense with the values obtained from literature. Several formulation have been introduced in the field of hard ceramics to evaluate fracture toughness using typical hardness indentation. However, Evan's equation, one of the adopted relations in the SiAlON field, is used in the present study, which can be written as follows:

$$K_{IC} = 0.48\left(\frac{MCL}{d/2}\right)^{-1.5}\left(\frac{HV_{10\sqrt{d/2}}}{3}\right)$$

Where MCL stands for the maximum crack length initiated from the indentation, d is the average depression diagonal and HV_{10} is the Vickers harness value.

CHAPTER 4

RESULTS AND DISCUSSION

Considering the scope and objective of the research, monolithic and composite ceramics were synthesized based on the selected α-SiAlON composition, $\boldsymbol{Ca_{0.8}Si_{9.2}Al_{2.8}O_{1.2}N_{14.8}}$, using the steps explained in the experimental methodology section. In this chapter, the results obtained from the synthesis and characterization of monolithic α-SiAlON ceramics are presented, followed by those obtained from the SiAlON composites.

4.1 Synthesis of Monolithic α-SiAlON

The experimental sequence was carried out in two steps; in the first step monolithic α-SiAlONs (without any reinforcement) were sintered at two different temperatures i.e. 1500 °C and 1600 °C. At each temperature 10, 20 and 30 minutes holding times were used to obtained hard single phase α-SiAlON ceramics. The sintering parameters of the sample with best hardness were then used for the synthesis of composite ceramics to compensate for the fracture toughness loss resulted due to formation of single phase α-SiAlON ceramic.

The chemically balanced proportion of the starting powders used for the fabrication of monolithic α-SiAlON ceramic is shown in Table 6.

Table 6: Chemical composition of monolithic samples (wt. %)

Composition	CaO	Si_3N_4	AlN	SiO_2
$\boldsymbol{Ca_{0.8}Si_{9.2}Al_{2.8}O_{1.2}N_{14.8}}$	7.57	71.03	19.37	2.03

4.1.1 Sintering and Densification

The density of the sintered α-SiAlON monolithic samples are shown in Table 7 along with the sample names. The sample names correspond to the sintering temperature and holding time at which these samples were sintered. For instance; sample name 1510 corresponds to a sintering temperature of 1500 °C with 10 minutes holding time. Similarly, sample name 1630 relates to a sintering temperature of 1600 °C with 30 minutes holding time.

Table 7: Densities of monolithic α-SiAlONs

Sample Name	Density (g/cm^3)
1510	3.15
1520	3.15
1530	3.19
1610	3.18
1620	3.18
1630	3.20

It was seen that there is minor difference in the density of the samples sintered at the two considered temperatures indicating that consolidation was achieved thanks to the spark

plasma sintering technique. A slight decrease in density was found with decreasing the holding time particularly for sample sintered at 1500 °C.

4.1.2 Phase Analysis

The X-ray Diffraction patterns of samples sintered at 1500 °C and 1600 °C are shown in Figure 14 and Figure 15 respectively. It is apparent that in samples 1510 and 1610, some aluminum nitride (AlN) peaks are visible which are attributed to undissolved AlN at 10 min holding time. It means that some of the AlN present in the starting powders did not react completely. However, for larger holding time, sample 1530 and 1630, the AlN peaks disappeared, indicating a complete reaction of the starting powders yielding a single-phase monolithic α-SiAlON.

Another important observation was also noted that in sample 1510, AlN peaks were more prominent as compared to those present in sample 1610, indicating that at a lower temperature the dissolution of aluminum nitride was difficult. Although there was very little difference in the densities of the samples but again with increase in holding time at a given temperature a relative increase in density could also be attributed to the presence of AlN in samples sintered at less holding time.

The effect of temperature on formation of α-SiAlON using micron-sized starting powder with CaO as an additive was repeated in reference [31], where it was observed that at 1600 °C with 1 hour holding time complete dissolution of S_3N_4 and AlN took place to form single phase α-SiAlON. It is worth noting that the use of nano-sized starting powders allowed us to synthesize single phase α-SiAlON at lower temperature of 1500 °C with holding time of just 30 minutes. It should also be appreciated that the choice of CaO as an

additive also relaxed the sintering temperature due to its lower melting temperature which could help in dissolution of present nitrides at a relatively lower temperature.

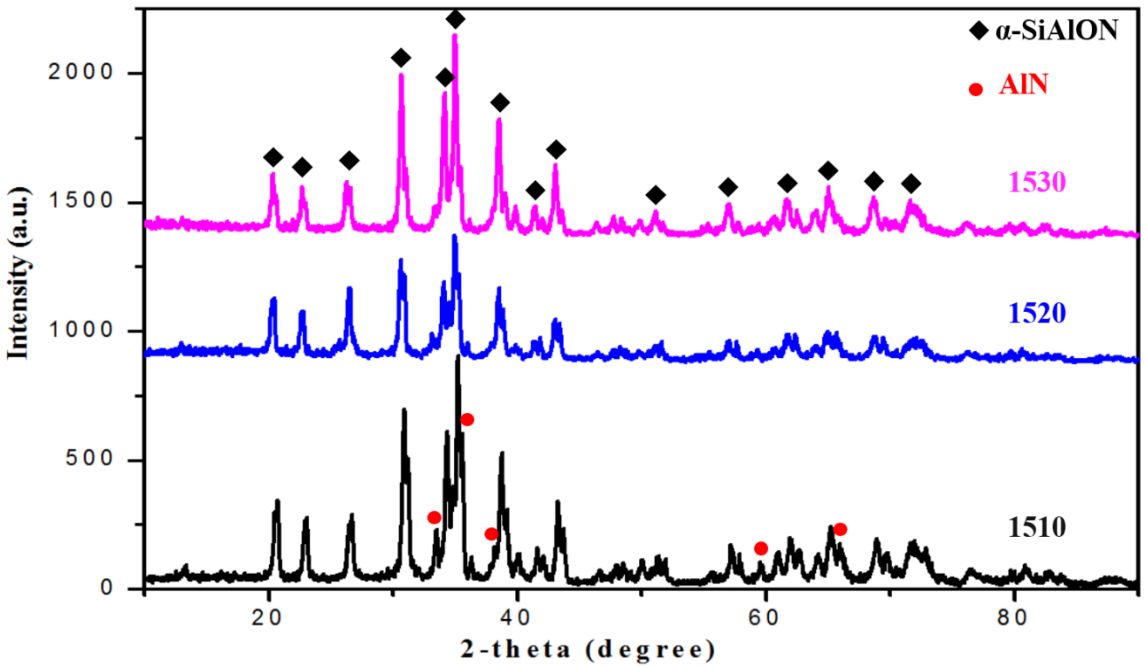

Figure 14: XRD of samples sintered at 1500 °C

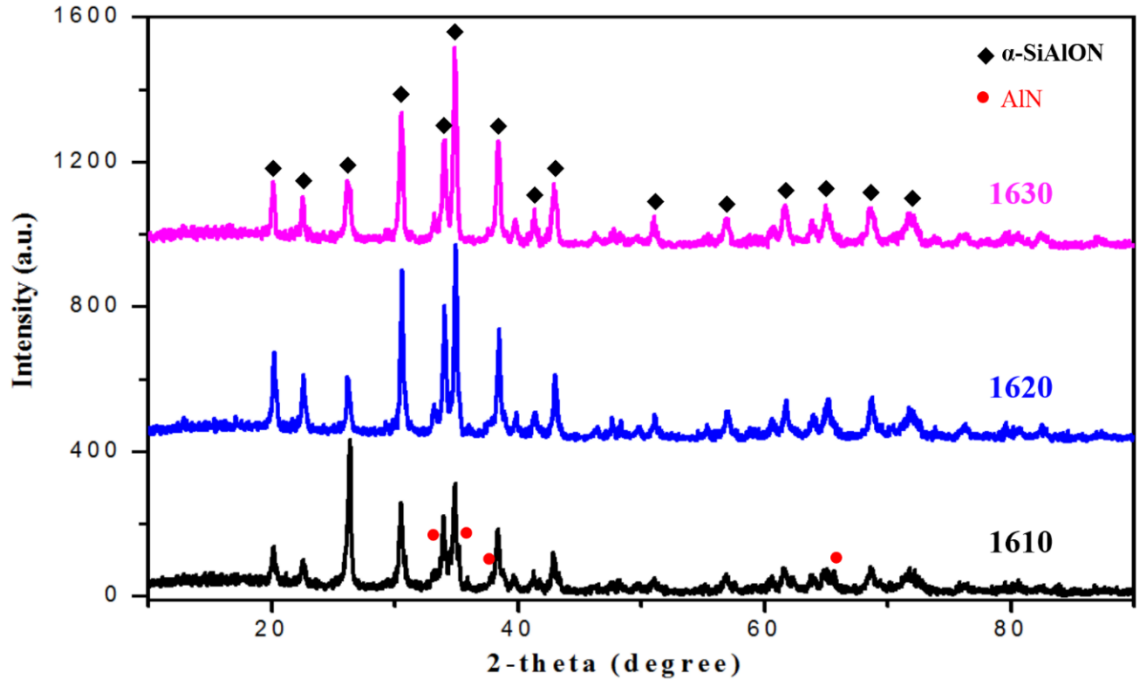

Figure 15: XRD of samples sintered at 1600 °C

4.1.3 Microstructural Analysis

The scanning electron microscope (SEM) images of all the six polished samples sintered at 1500 °C and 1600 °C with 10, 20 and 30 minutes holding time are shown in Figure 16. As illustrated from the SEM micrographs, the amount of porosity was found to be reduced with increased holding time at a particular temperature. It could also be noted that the content of porosity in sample 1510, Figure 16 (a), was higher than the sample 1610, Figure 16 (d). The presence of porosity in samples sintered with less holding time at a particular temperature could also be attributed to the very little relative decrease in the density of sintered samples with decreasing holding time. The reduction in amount of porosity with increasing holding time was also in agreement with phase analysis data, as it was shown earlier that some amount of undissolved aluminum nitride was found in samples sintered with less holding time at a given temperature.

SEM micrographs of samples sintered at 1500 °C and 1600 °C with 30 minutes holding time are shown in Figure 17. Single phase equiaxed α-SiAlON grains could be seen in both micrographs as confirmed by the x-ray diffraction analysis. The average grain size for sample sintered at 1500 °C with 30 min holding time (1530), Figure 17 (a), was about three times finer than that of the sample sintered at 1600 °C with 30 min holding time (1630), Figure 17 (b), indicating that grain growth took place at 1600 °C, as reported also elsewhere[42].

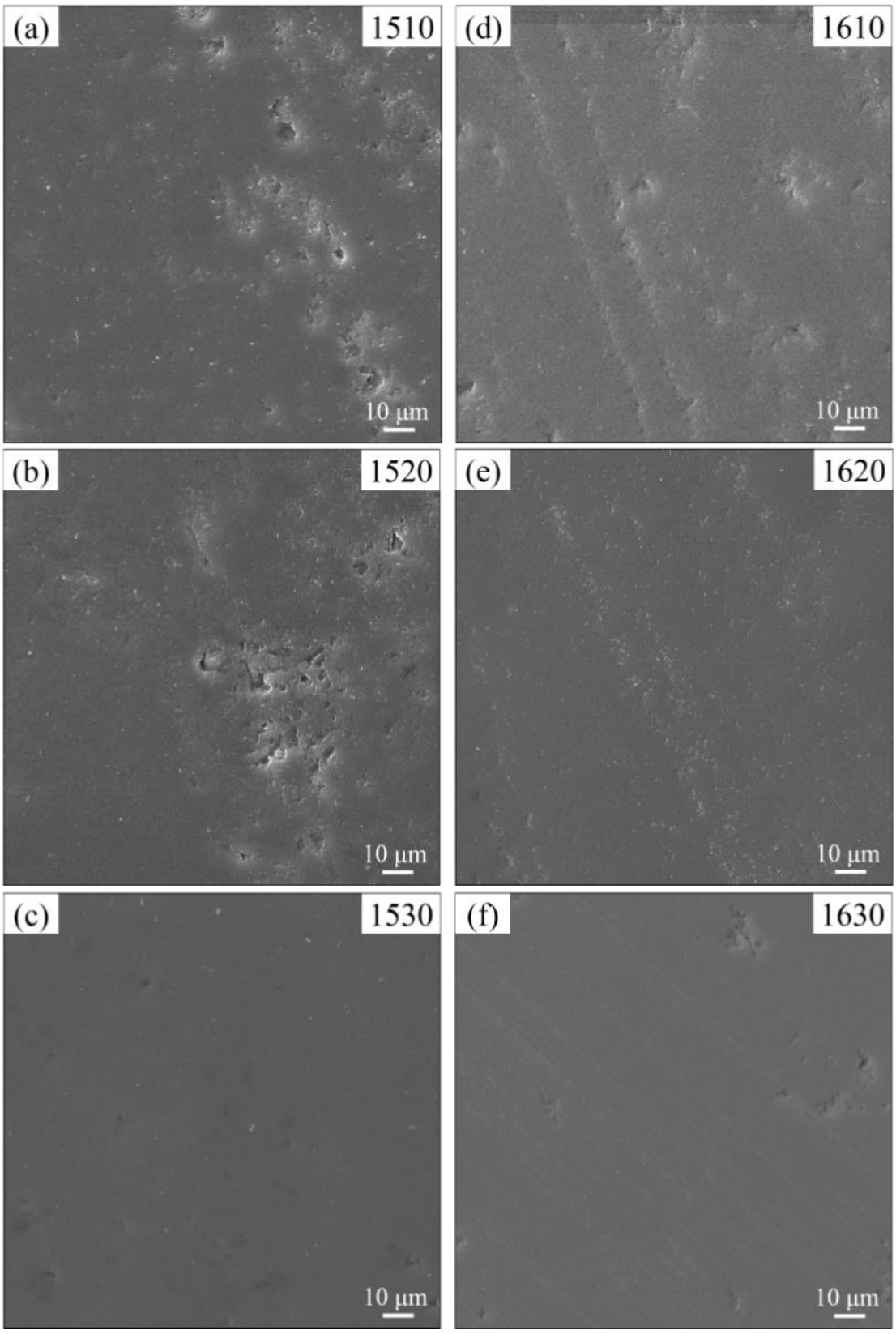

Figure 16: SEM micrographs of samples sintered at 1500 °C with (a) 10, (b) 20, (c) 30 min holding time and samples sintered at 1600 °C with (d) 10, (e) 20, (f) 30 min holding time

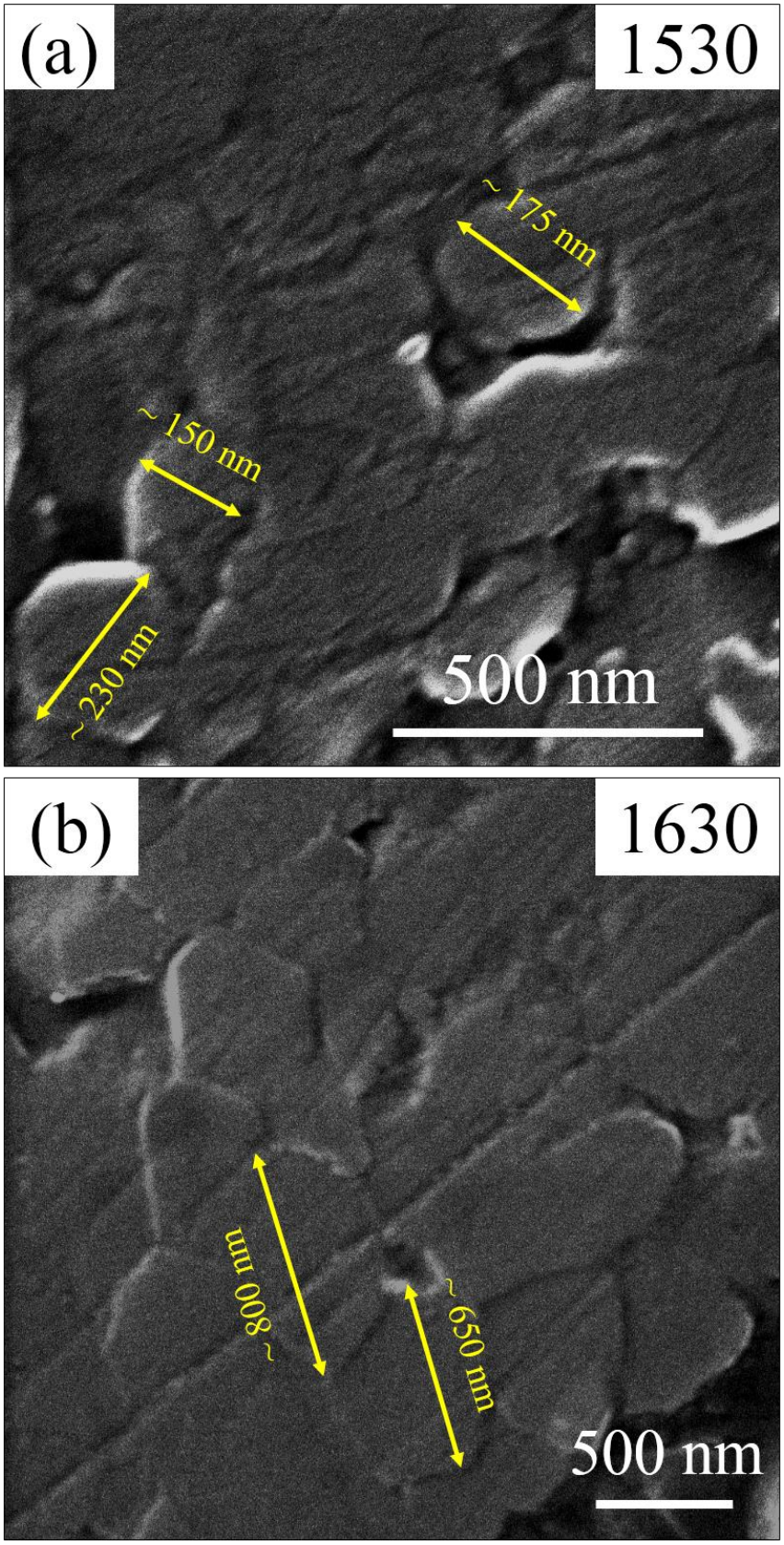

Figure 17: Grain size of monolithic α-SiAlON sintered at (a) 1500 °C and (b) 1600 °C with 30 min holding time

4.1.4 Mechanical Properties

Table 8 depicts the mechanical properties, hardness and fracture toughness, of the prepared monolithic α-SiAlON samples. It was found that the hardness and fracture toughness for the samples sintered at both temperatures was showing an increasing trend with the increase in holding time, except for sample 1620 where the fracture toughness decreased. It is also clear that with increase in sintering temperature, i.e. from 1500 °C to 1600 °C, the hardness slightly decreased while the fracture toughness increased.

Table 8: Mechanical properties of monolithic α-SiAlONs

Sample Name	Hardness HV_{10} (GPa)	Fracture Toughness ($MPa.m^{1/2}$)
1510	19.83 ± 0.35	4.37 ± 0.41
1520	20.07 ± 0.26	4.67 ± 0.36
1530	21.06 ± 0.42	7.29 ± 1.33
1610	19.27 ± 0.64	9.55 ± 1.23
1620	20.13 ± 0.52	7.80 ± 2.30
1630	20.50 ± 0.41	9.65 ± 2.30

The mechanical properties, particularly hardness, of the samples could easily be associated to the x-ray diffraction pattern. The relatively high values of hardness for sample 1530 and 1630 as compared to their counterparts sintered at same temperature but less holding time could be attributed to the presence of single phase α-SiAlON in samples 1530 and 1630 as

this is the hardest phase in SiAlONs. While for samples sintered with lower holding times the presence of AlN, due to incomplete reaction, as depicted by XRD, could be attributed to relatively lower hardness values.

The increased hardness (21.06 GPa, Hv_{10}) of the sample 1530, sintered at 1500 °C with 30 min holding time, as compared to the hardness value (20.05 GPa, Hv_{10}) of the sample 1530, sintered at 1600 °C with 30 min holding time, could be explained by considering very fine microstructure of sample 1530 as compared to larger grain sizes in sample 1630. The higher values of fracture toughness (9.65 $MPa.m^{1/2}$) for sample 1630 could also be attributed to the grain size as depicted in the micrographs, Figure 17 (a) and (b). The increased grain size could provide self-toughening mechanism by crack deflection in intergranular mode of crack propagation.

The behavior of hardness and fracture toughness with respect to increase in holding time at the two respective temperatures is also quite apparent in the graphical form in Figure 18 and Figure 19 respectively.

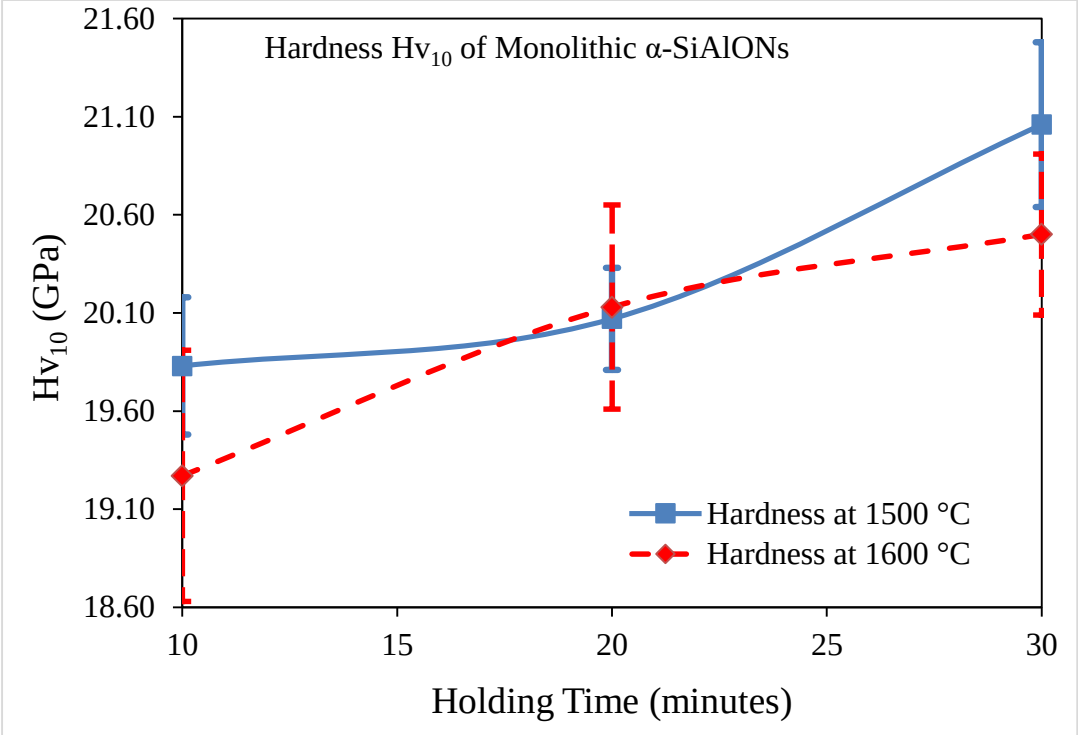

Figure 18: Hardness of monolithic α-SiAlON sintered at different temperatures & holding times

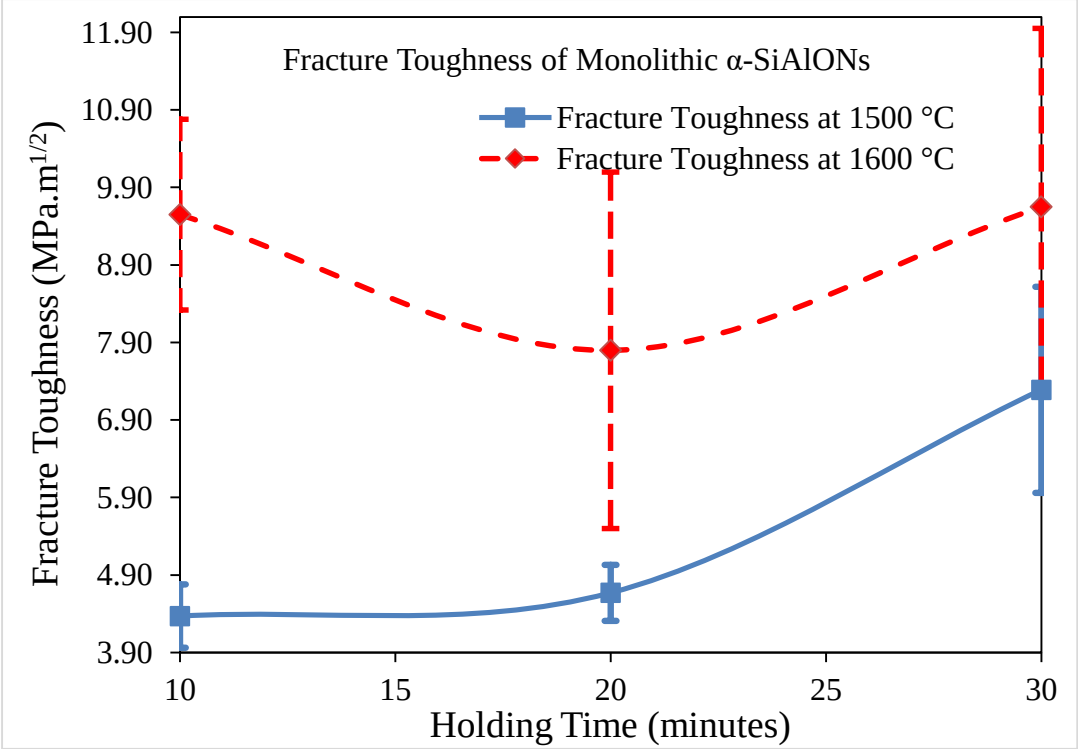

Figure 19: Fracture toughness of monolithic α-SiAlON sintered at different temperatures & holding times

The fractographs of samples sintered at 1500 °C with holding time 10, 20 and 30 minutes are shown in Figure 20 (a), (b) and (c) respectively. Similarly the fractographs for samples sintered at 1600 °C with 10, 20 and 30 minutes holding time are shown in Figure 20 (d), (e) and (f) respectively.

The fracture surfaces of sample 1510 and 1610 show some voids or open spaces which could be associated with relatively low density of these samples and incomplete reaction due to the presence of undissolved aluminum nitride. It should also be noted that these voids were more prominent in samples 1510 than that in sample 1610 which could explain higher fracture toughness of sample 1610. These types of voids were also present in sample 1520 but with increasing holding time no such voids were seen which could depict the relative increase in density and hardness with increase in holding time at a particular temperature

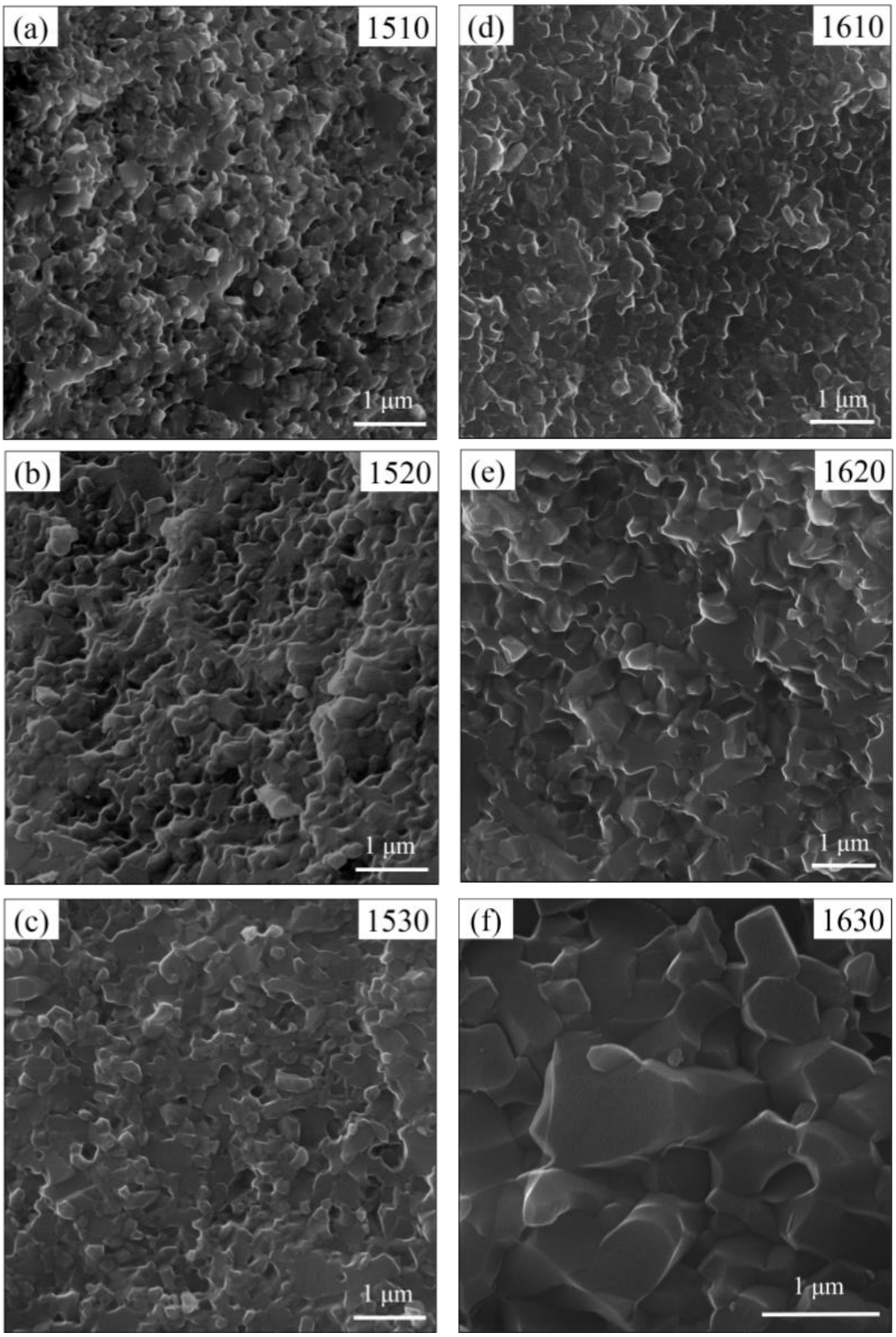

Figure 20: SEM-fractographs of samples sintered at 1500 °C with (a) 10, (b) 20, (c) 30 min holding time and samples sintered at 1600 °C with (d) 10, (e) 20, (f) 30 min holding time

By looking carefully the fracture surfaces of sample 1530 and 1630 it could be easily said that sample 1530, Figure 21 (a), has a harder fracture due to finer average grain size as compared to the sample 1630. Higher amount of grain elongation in sample 1630, Figure 21 (b), was one of the reasons for the increased fracture toughness, in addition to pulling out observed in this sample [52]. The high heating rate, 100 °C/min, used in processing using spark plasma sintering could also play an important role in the elongation of α-SiAlON grains providing self-toughening in these ceramics [26]. For sample 1530 the elongation of grains was also observed but it was not as prominent as in sample 1630, Figure 21 (b).

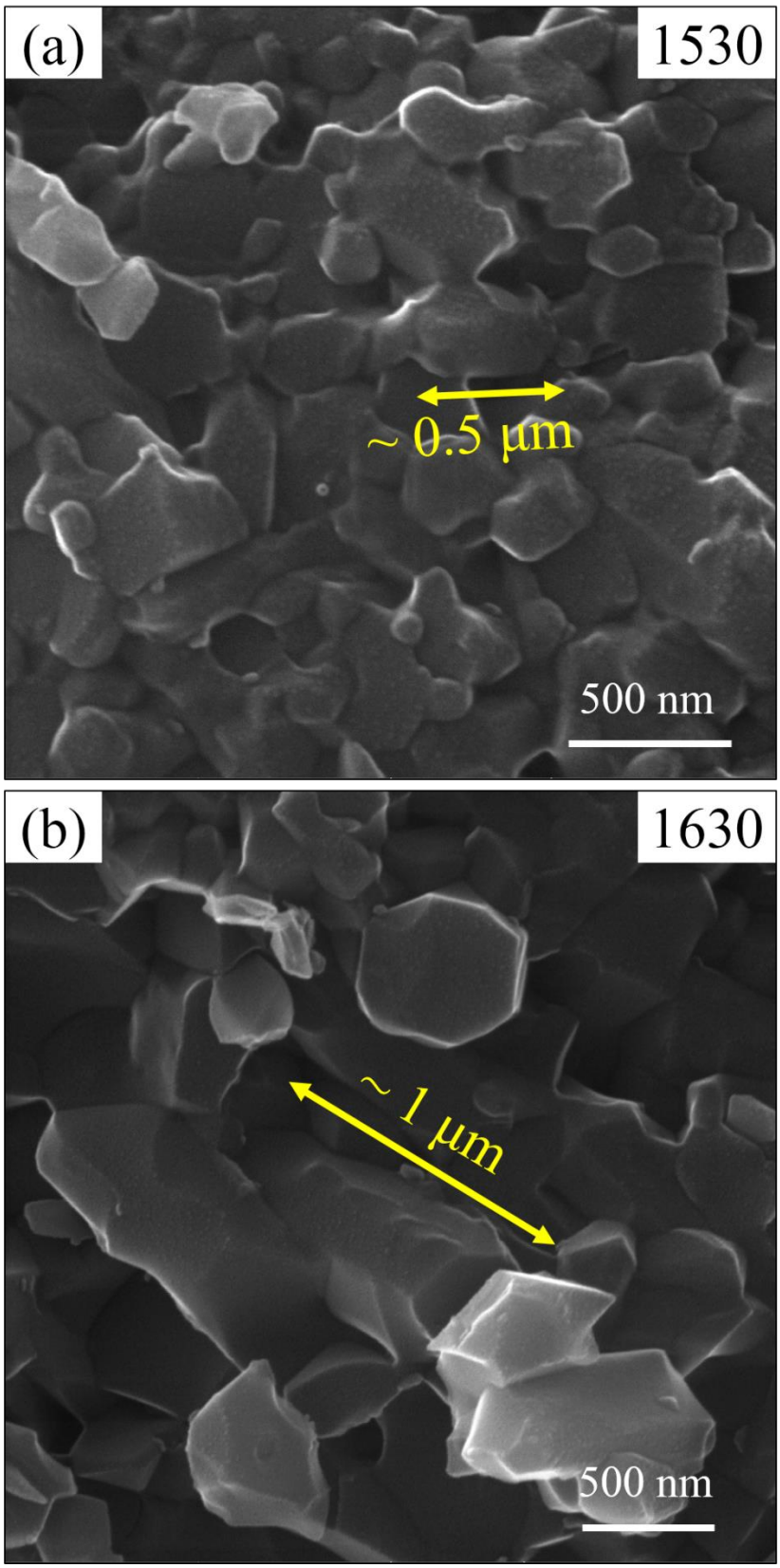

Figure 21: Elongation of α-SiAlON grains in Samples (a) 1530 and (b) 1630, sintered at 1500 °C and 1600 °C respectively with 30 min holding time

On the basis of mechanical properties, microstructural analysis and phase investigation it is evident that the hardness of sample 1530 is highest with modest fracture toughness, and has a single phase α-SiAlON. Sample 1530 was, therefore, considered as a matrix for developing α-SiAlON composites by adding reinforcements to enhance the fracture toughness. The following sintering parameters; Temperature-1500 °C, Holding time-30 minutes, Heating Rate- 100 °C /min, Environment-Vacuum and Pressure-50 MPa were selected for the synthesis of α-SiAlON ceramics composites based on these remarks:

- Dense single phase α-SiAlON was obtained in sample 1530 (sintered at 1500 °C and held for 30 at sintering temperature).
- Sample 1530 exhibited the best hardness value.
- Although sample 1530 has relatively lower fracture toughness than sample 1630 but it could be compensated by the inculcation of reinforcements.
- The sintering temperature for sample 1530 was 100 °C less than that of sample 1630, yielding less energy consumption and more economic processing.

4.2 Synthesis of α-SiAlON Composites

Three different types of reinforcing particles were added to the monolithic α-SiAlON in order to further enhance the mechanical properties of SiAlON ceramics (particularly fracture toughness). These three reinforcements were Silicon Carbide-SiC (μm), Tungsten Carbide-WC (μm), and nano Silicon Carbide-SiC (nm), and the amounts were 10, 20 and 30 weight percent (wt. %). The discussion related to these three reinforcements is divided as follows:

- Micron Silicon Carbide-SiC (μm)/α-SiAlON Composite
- Nano Silicon Carbide-SiC (nm)/α-SiAlON Composite
- Tungsten Carbide-WC (μm)/α-SiAlON Composite

4.2.1 Micron Silicon Carbide-SiC (μm)/α-SiAlON Composite

Table 9 shows the sample name and amount of SiC (μm) added in each batch of the matrix powder. The sample names depict the sintering temperature and the amount of reinforcement added, for instance the sample named 1530-1SiC(μm) means sample sintered at 1500 °C with 30 min holding time containing 10 wt. % of SiC (μm).

Table 9: Wt. % of SiC (μm) in each batch of the matrix for the powder composites

Sample Name	Matrix	SiC (μm) wt. %
1530-1SiC(μm)	α-SiAlON	10
1530-2SiC(μm)	α-SiAlON	20
1530-3SiC(μm)	α-SiAlON	30

Sintering and Densification

The samples containing 10, 20 and 30 wt. % of SiC were synthesized following the experimental procedure mentioned earlier and, the experimental and calculated densities were determined and displayed in Table 10. It is evident that complete densification for all the samples was achieved which could be attributed to uniform and homogeneous dispersion of reinforced particles [53].

Table 10: Densification of SiC (μm)/α-SiAlON composite ceramics

Sample Name	Experimental Density (g/cm^3)	Calculated Density (g/cm^3)	Percentage Densification
1530	3.19	--	--
1530-1SiC(μm)	3.1915	3.1918	99.99
1530-2SiC(μm)	3.1925	3.1933	99.97
1530-3SiC(μm)	3.1932	3.1946	99.95

Microstructural Analysis

Figure 22 (a), (b) and (c) show the back scattered electron images of polished samples along with EDS mapping, showing the distribution of SiC (μm) in α-SiAlON matrix, containing 10, 20 and 30 wt. % of SiC (μm) sintered at 1500 °C with 30 min holding time.

It was illustrated from the micrographs that no porosity was found in the composite samples even with 30 wt. % addition of SiC (μm). This was also depicted from the densification data where almost 100 % densification has been achieved for the all the three composite samples.

The homogeneous distribution of SiC (μm).could be depicted from the distribution of carbon shown along with the back scattered electrons (BSE) micrographs for each of the three composites. No evidence of agglomeration was found in any of the three composite samples which is in accordance with no indication of porosity content (from the micrographs) and complete densification of all the composite samples.

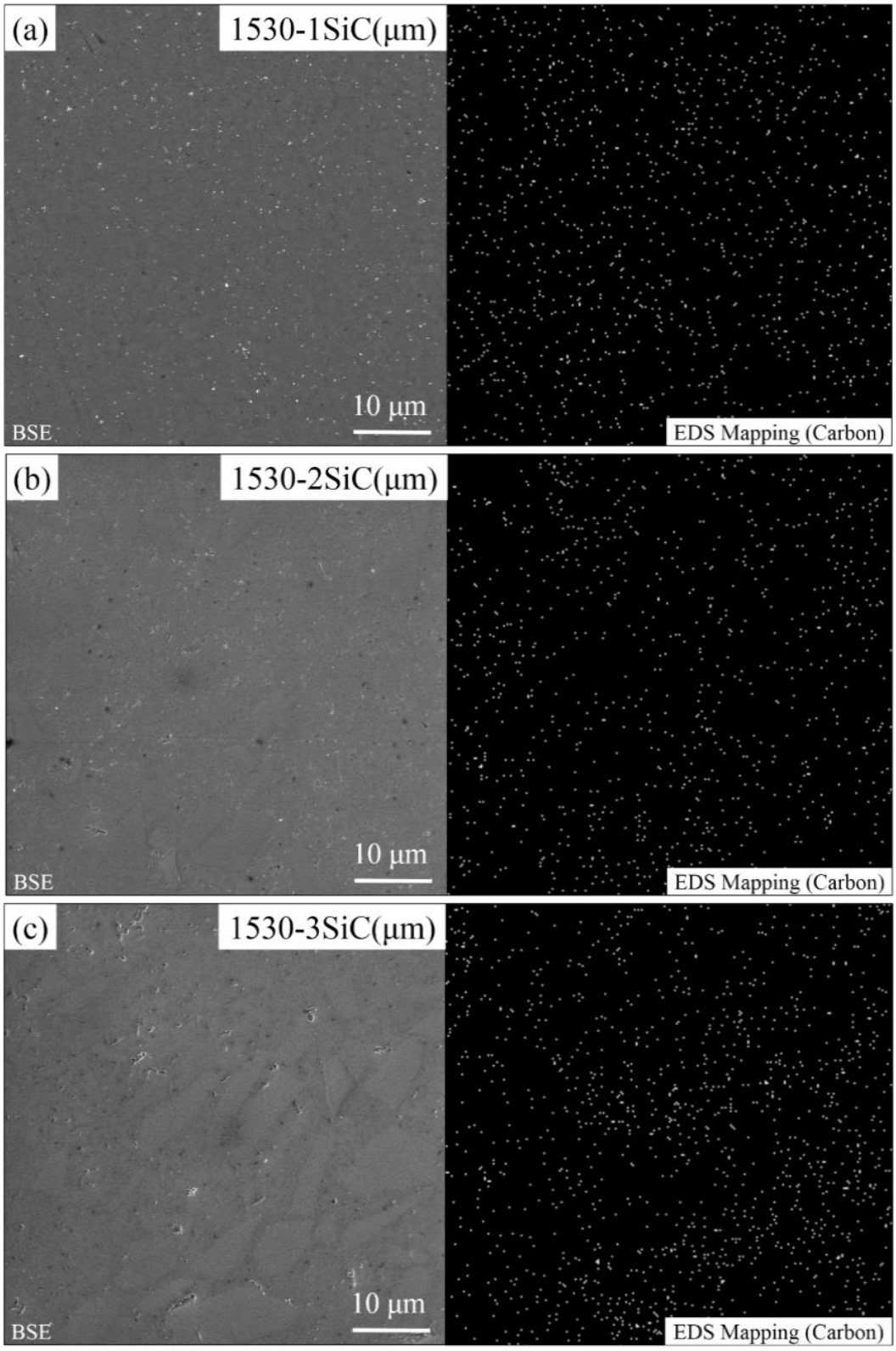

Figure 22: BSE micrographs and EDS mapping of samples with (a) 10 wt. %, (b) 20 wt. % and (c) 30 wt. % of SiC (μm) in α-SiAlON matrix

Phase Analysis

Figure 23 shows the x-ray diffraction pattern of monolithic α-SiAlON, sample 1530, along with the patterns of 10 wt. %, 20 wt. % and 30 wt. % SiC(μm) /α-SiAlON composite ceramics. In zero wt. % SiC sample, single phase α-SiAlON was found. It was observed that the SiC peaks intensity was increasing in samples with higher amount of the particle reinforcements. Moreover no other peaks were found other than the inculcated SiC particles and α-SiAlON matrix, indicating that there was no chemical interaction between the matrix and the second phase SiC (μm) particles [26]. The α-SiAlON peaks were also prominent in x-ray diffraction of each composite ceramic.

It should also be noted that, due to the use of CaO as additive and nano size starting powders resulting in lower processing temperature, no evidence of phase transformation of SiC was found which could otherwise be detrimental to the properties of the composites [31]. α-SiC in the final assembly remained the same as the introduced SiC because of the thermodynamic stability of .α-SiC below 2100 °C [48].

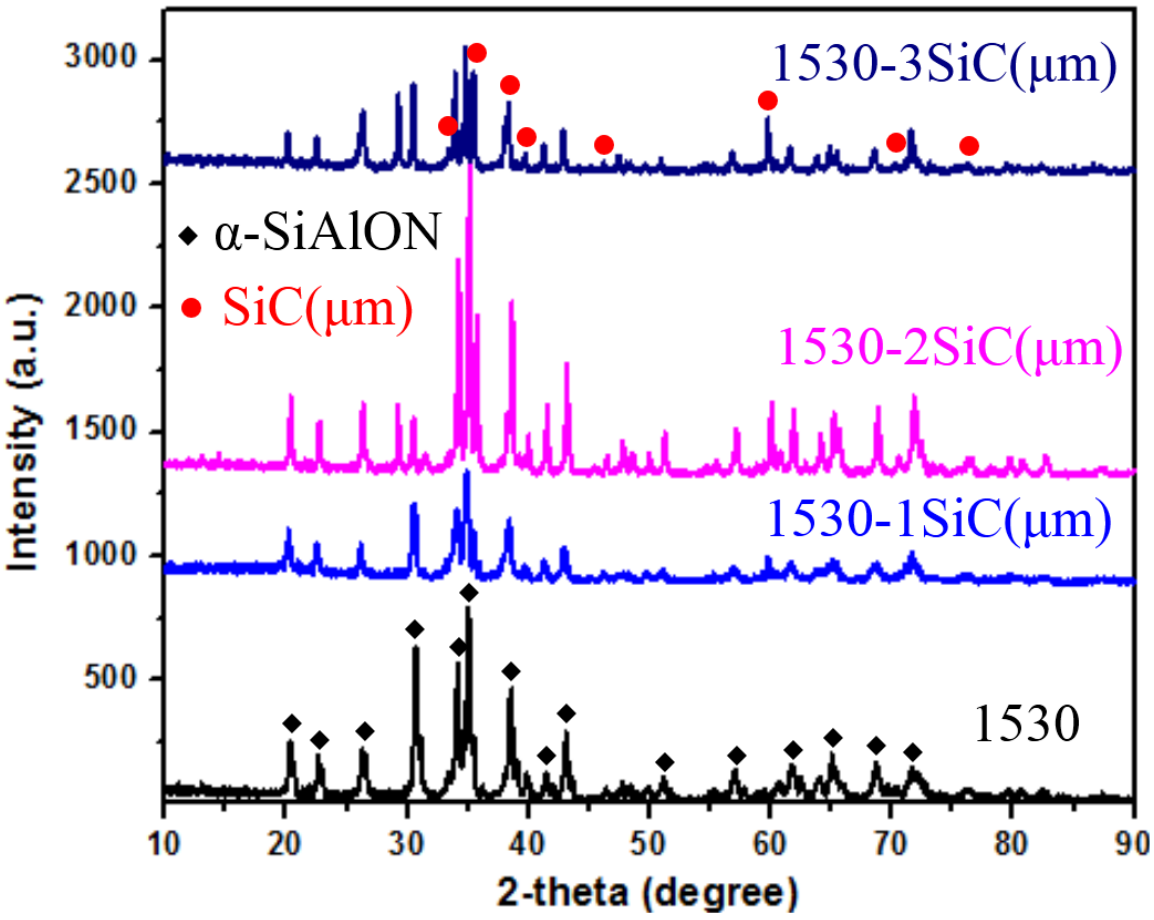

Figure 23: XRD of monolithic α-SiAlON, 10 wt. %, 20 wt. % and 30 wt. % SiC(μm)/α-SiAlON Composites

Mechanical Properties

The mechanical properties, hardness and fracture toughness, of the reinforced nano-composite ceramics are shown in Table 11. With the addition of SiC (μm) tremendous results were obtained as compared to the previously reported results. In most of the available literature, people were sintering SiAlONs at higher temperature while in present case very hard and tough ceramics were fabricated at relatively lower temperature. The higher hardness with increase in amount of SiC reinforcements was attributed to the higher hardness of SiC itself [48]. With 30 wt. % addition of SiC (μm) in monolithic α-SiAlON, an increase of about 16 % and 63 % was achieved in the values of hardness and fracture toughness respectively, which was undoubtedly a great success achieved in the present work.

Table 11: Mechanical properties of SiC (μm)/α-SiAlON composite ceramics

Sample Name	Hardness HV_{10} (GPa)	Fracture Toughness ($MPa.m^{1/2}$)
1530	21.06 ± 0.42	7.29 ± 1.33
1530-1SiC(μm)	21.47 ± 0.27	9.10 ± 0.71
1530-2SiC(μm)	23.12 ± 0.44	10.51 ± 0.34
1530-3SiC(μm)	24.53 ± 0.23	11.86 ± 0.54

This behavior of SiC (μm) particles addition will be explained in the coming sections with the help of SEM micrographs, indentation and crack propagation images as well as by considering the densification percentage and phase analysis. The contribution of SiC (μm) reinforcements is also shown in a graphical in Figure 24.

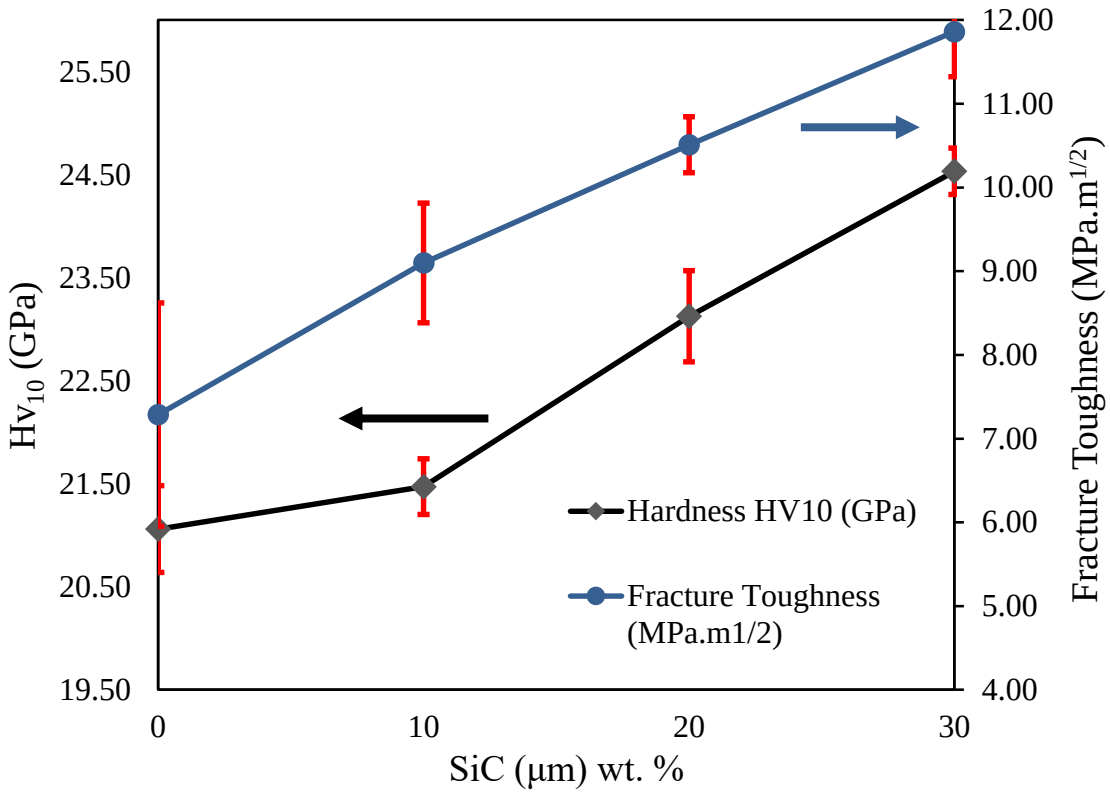

Figure 24: Trend of mechanical properties of SiC (µm)/α-SiAlON composite ceramics

The backscattered electron microscopy images of the fracture surfaces of monolithic α-SiAlON (sample 1530), SiC/α-SiAlON composites with 10, 20 and 30 wt. % of SiC (μm) are shown in Figure 25 (a), (b), (c) and (d) respectively. A sharp and distinct contrast between α-SiAlON matrix and Silicon Carbide reinforcements was not detected because of only one atomic number difference between Carbon (atomic number = 6) and Nitrogen (atomic number = 7) elements [54]. As an example few probable SiC particles were encircled in the fracture surface images. If observed closely one can see the light grayish or whitish SiC particles dispersed homogenously in the matrix Figure 25 (b), (c) and (d). The high hardness of the composite ceramics could be attributed to homogeneous dispersion of the second phase in the matrix.

The arrows shown in Figure 25 (d) in sample 1530-3SiC(μm) represent the friction pulling out and grain tearing mechanisms which were suggested as one of the most prominent reasons of enhanced hardness and fracture toughness in composite ceramics with increasing the amount of SiC (μm) [55]. In contrast sample 1530 (with no reinforcements) with relatively lower fracture toughness did not show this type of behavior very prominently, instead it exhibited a more intergranular type of fracture. The coarse microstructure features of the fracture surface of the composite ceramics particularly of sample 1530-3SiC(μm) also explained the toughening of the composite samples [56].

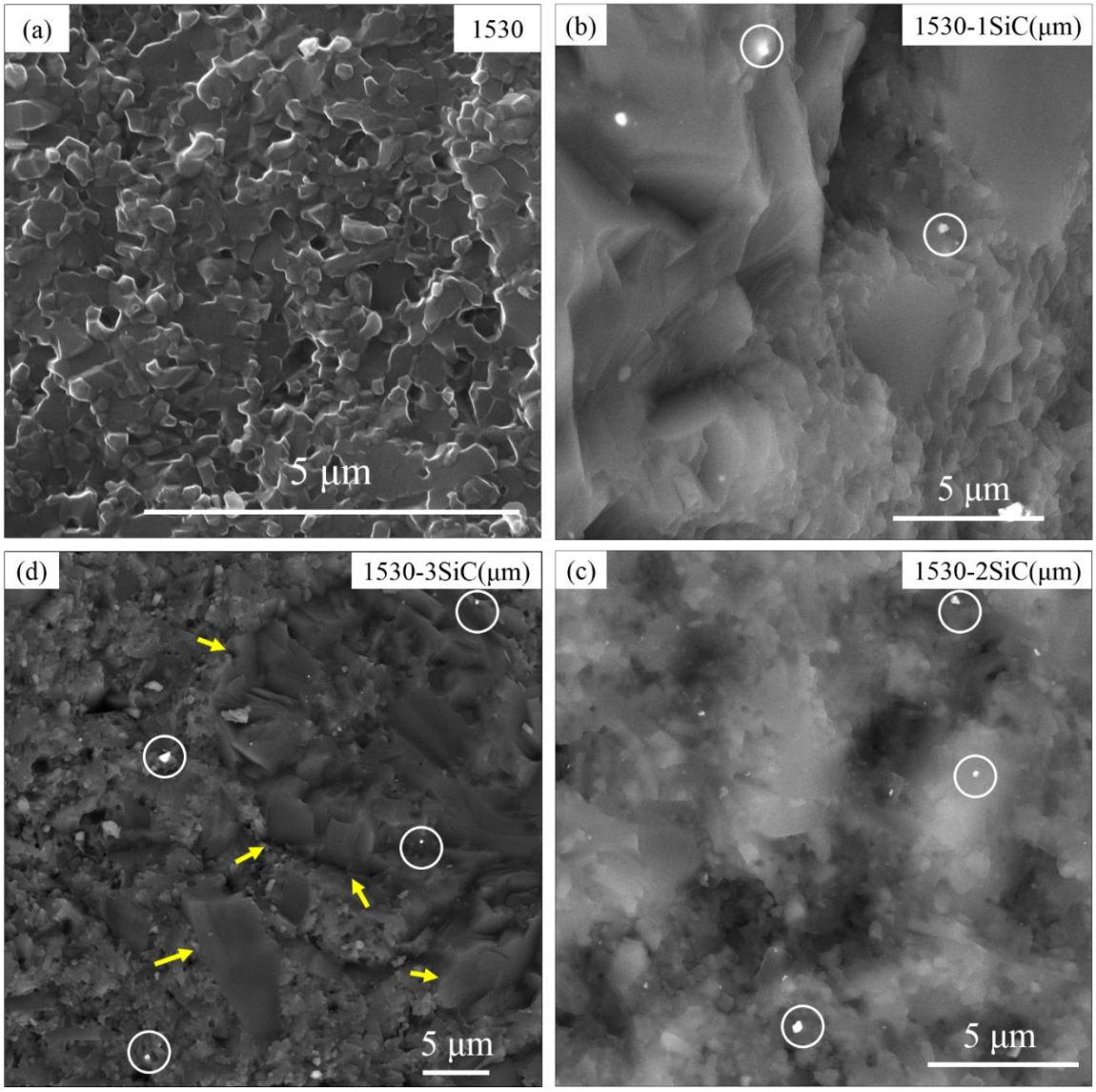

Figure 25: BSE-Fracture surfaces of (a) monolithic α-SiAlON, (b) 10 wt. % (c) 20 wt. % (d) 30 wt. % SiC(µm)/α-SiAlON composites

Figure 26 (a, b) and (c, d) show the Vickers indentation along with the crack propagation in monolithic α-SiAlON sample (1530) and sample with 30 wt.% of SiC (μm) (1530-3SiC(μm)) respectively. It was illustrated from the micrographs that sample 1530 showed a fast crack propagation as the crack was not deflected on its way, Figure 26 (b). But from the crack propagation in sample 1530-3SiC(μm), it was very obvious that crack was deflected, Figure 26 (d). In the higher magnification image taken from Figure 26 (d), crack bridging phenomenon was also observed carefully. These phenomenon of crack deflection, where the direction of crack propagation is forced to change to an angle of less than 90° from an angle perpendicular to the direction of applied stress thereby slowing down the propagation of crack by reducing the stress intensity at the crack tip [57], and crack bridging, where the stress intensity at the crack is reduced by bowing of the crack and the grains remain intact behind the crack [58], greatly enhanced the fracture toughness of the composite ceramics. The coarse microstructure found in the fracture surfaces of the composite samples could also contribute to enhancement of fracture toughness by encouraging the development of very considerable bridging zones [59].

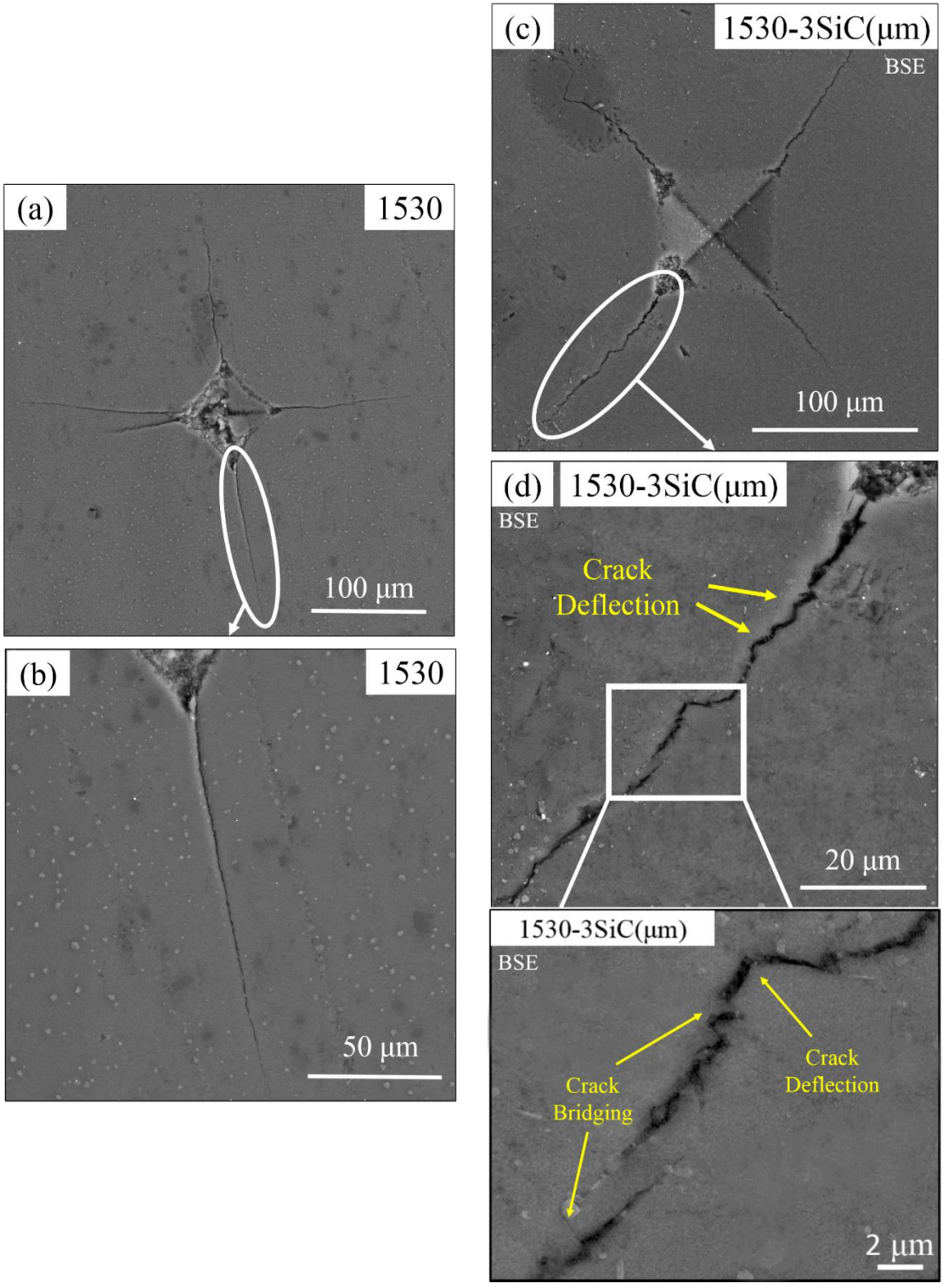

Figure 26: BSE-Comparison of indentation and crack propagation in (a, b) monolithic α-SiAlON and (c, d) 30 wt. % SiC (µm)/α-SiAlON composite

The back scattered electron microscopy image of the un-etched polished sample 1530-2SiC(μm) is shown in Figure 27 (a, b). The magnified image (b) showed the presence of hard SiC (μm) particle which forced the crack to change its direction hence making the propagation of crack slow. The interface between the matrix and the reinforcement particle also plays an important role in toughening of ceramics [60]. Weak interface between the matrix and the reinforcing particles makes the crack pass via interface as crack always likes to travel through a less resistive path. It seems from Figure 27 (b) that probably there existed a weak interface between SiC (μm) particles and α-SiAlON matrix allowing the crack to change its course. The deflection of crack and zig-zag behavior of the crack propagation also explained the increased fracture toughness [61].

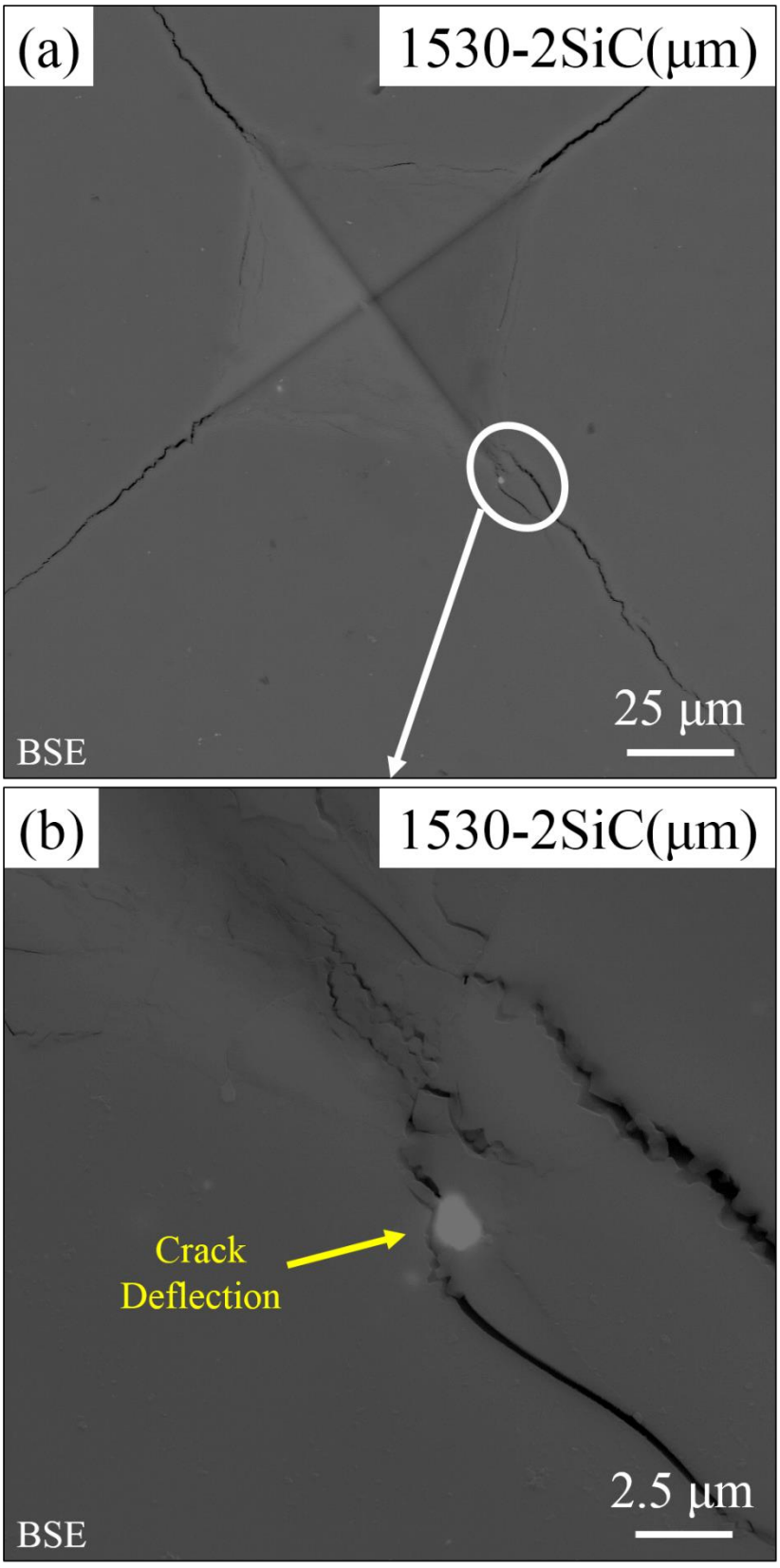

Figure 27: BSE-Indentation and crack in 20 wt. % SiC (μm)/α-SiAlON composite

4.2.2 Nano Silicon Carbide-SiC (nm)/α-SiAlON Composite

Table 12 shows the sample name and amount of SiC (nm) added in each batch of the matrix powder according to the balanced chemical equilibrium depending upon the general formula of the matrix, $Ca_{0.8}Si_{9.2}Al_{2.8}O_{1.2}N_{14.8}$ .Sample name corresponds to the sintering condition and the amount of reinforcement added.

Table 12: Wt. % of SiC (nm) in each batch of the matrix for the powder composites

Sample Name	Matrix	SiC (nm) wt. %
1530-1SiC(nm)	α-SiAlON	10
1530-2SiC(nm)	α-SiAlON	20
1530-3SiC(nm)	α-SiAlON	30

Sintering and Densification

After sintering and cleaning of samples, in accordance with the experimental procedure, the density of the composite samples reinforced with SiC (nm) was measured and calculated as illustrated in Table 13.

Table 13: Densification of SiC (nm)/α-SiAlON nano-composite ceramics

Sample Name	Experimental Density (g/cm^3)	Calculated Density (g/cm^3)	Percentage Densification
1530	3.19	--	--
1530-1SiC(nm)	3.17	3.19	99.42
1530-2SiC(nm)	3.13	3.19	98.27
1530-3SiC(nm)	3.14	3.20	98.27

Sample with 10 wt. % addition of second phase, 1530-1SiC(nm), exhibited full densification. There was a decrease in percentage densification of sample with 20 and 30 wt. % of SiC (nm), sample 1530-2SiC(nm) and sample 1530-3SiC(nm), which could probably be attributed to agglomeration of SiC nano particles in α-SiAlON matrix [26] [62], and will be demonstrated in the coming sections.

Phase Analysis

Figure 28 shows the x-ray diffraction pattern of monolithic α-SiAlON, sample 1530, along with the patterns of 10 wt. %, 20 wt. % and 30 wt. % SiC(nm)/α-SiAlON composite ceramics. Sample with zero wt. % SiC (nm), sample 1530 produced single phase α-SiAlON. The α-SiAlON peaks were also very prominent in x-ray pattern of each composite ceramic. Samples with increased amount of SiC (nm) particles showed higher peak intensities for the reinforced SiC (nm) which is a typical behavior in dual phase composites. Moreover no other peaks were found other than the inculcated SiC (nm) particles and α-SiAlON matrix which depicted that there was no chemical interaction between the matrix and the second phase SiC (nm) particles [26].

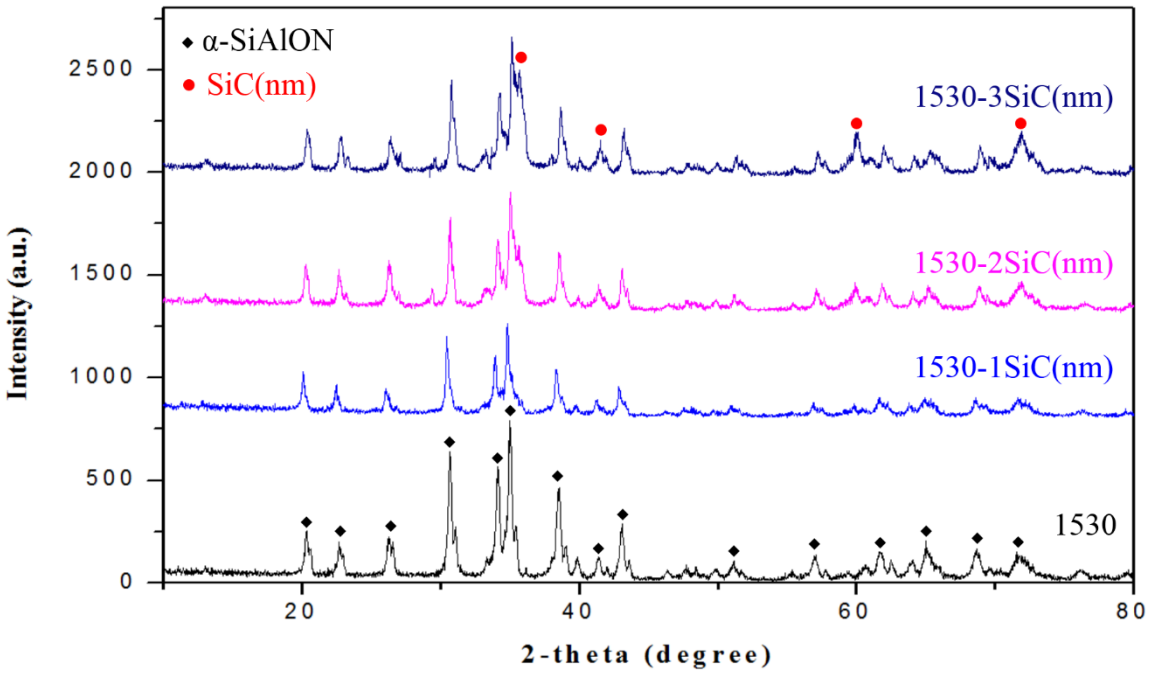

Figure 28: XRD of monolithic α-SiAlON, 10 wt. %, 20 wt. % and 30 wt. % SiC(nm)/α-SiAlON nano-composites

Microstructural Analysis

Figure 29 (a), (b) and (c) shows the back scattered electron images of polished samples along with EDS mapping, showing the distribution of SiC (nm) in α-SiAlON matrix, containing 10, 20 and 30 wt. % of SiC (nm) sintered at 1500 °C with 30 min holding time. SiC (nm) particles were difficult to see because of low contrast (low z-value difference between N and C elements) between SiAlON and Silicon Carbide [54]. It was illustrated from the micrographs that porosity content for composite samples was increased with increase in amount of SiC (nm).

The dispersion of SiC (nm).in the matrix was represented from the distribution of carbon showed along with the BSE micrographs for each of the three composites. It was observed that some areas of the maps were empty while at some regions clusters were found particularly in sample with 30 wt. % of SiC (nm). These observation from BSE-micrographs and EDS-mapping were associated to the densification data where a relative decrease in densification was found with increase in SiC (nm) amount [26, 62].

Figure 30 also shows the agglomerated clusters of SiC (nm) in the matrix along with porosities found in the sample. Here it should be noted that the contrast was set up manually after taking back scattered image to show the agglomeration of particles in the composite samples, as it was previously stated that auto-contrast for such type of composite ceramics could not be set easily using the backscatter detector in scanning electron microscope.

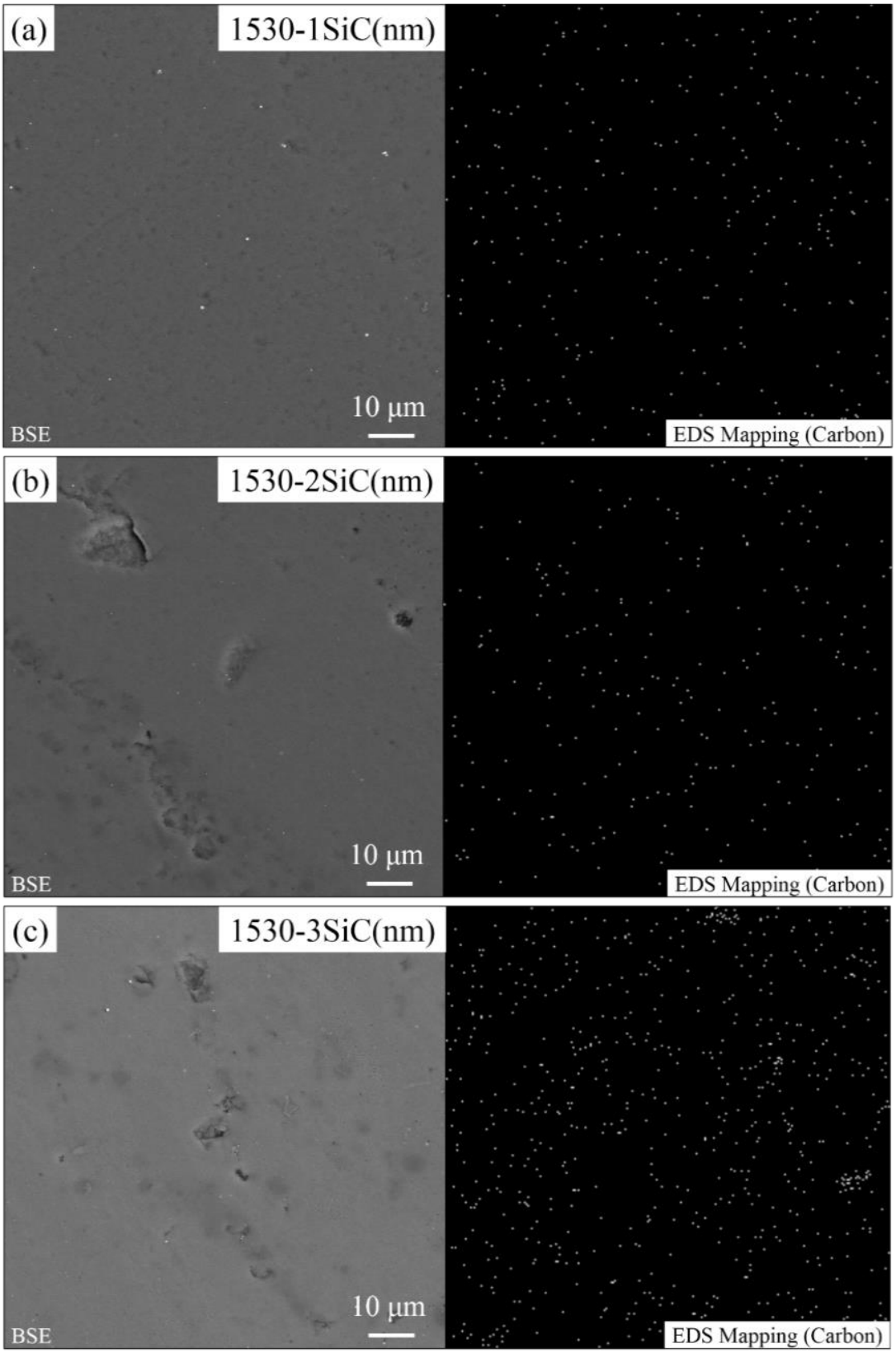

Figure 29: BSE micrographs and EDS mapping of samples with (a) 10 wt. %, (b) 20 wt. % and (c) 30 wt. % of SiC (nm) in α-SiAlON matrix

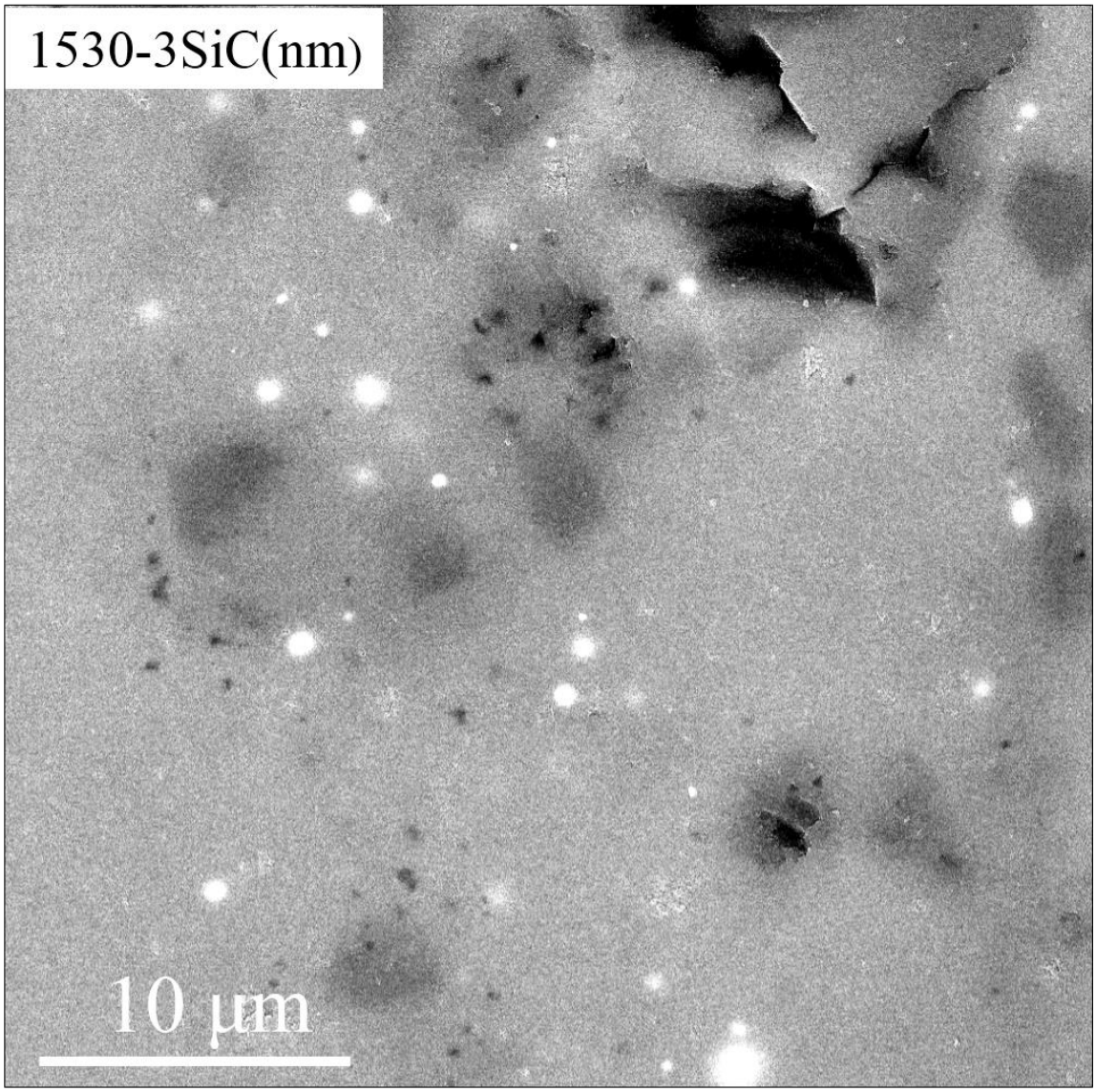

Figure 30: Particulate agglomerations in form of clusters

Mechanical Properties

The mechanical properties, hardness and fracture toughness, of the reinforced nano composite ceramics are shown in Table 14. It was observed that the hardness and fracture toughness of the nano composite ceramics decreased with the increase in amount of reinforcements. The deterioration of hardness values could be attributed to relatively lower density of the composites. It should be noted that sample with 10 wt. % of SiC (nm), 1530-1SiC(nm), was presenting a little increase in hardness value and full densification as well. While poor fracture toughness of the nano composite ceramics as compared to the monolithic α-SiAlON ceramic, sample 1530, could probably be associated with the agglomeration of second phase particles [62] [53].

Table 14: Mechanical properties of SiC (nm)/α-SiAlON nano-composite ceramics

Sample Name	Hardness HV_{10} (GPa)	Fracture Toughness ($MPa.m^{1/2}$)
1530	21.06 ± 0.42	7.29 ± 1.33
1530-1SiC(nm)	21.44 ± 0.27	5.95 ± 1.26
1530-2SiC(nm)	20.74 ± 0.78	4.86 ± 0.55
1530-3SiC(nm)	20.01 ± 0.31	3.38 ± 0.24

The comparison of the mechanical properties with increase in amount of SiC (nm) is also shown in Figure 31. Very prominent decrease in fracture toughness with relatively small decrease in hardness was seen with the increase in amount of nano silicon carbide. For fracture toughness it should be noted that the error bar of sample 1530-1SiC(nm) was coinciding with the error bar of sample 1530 which depicted no or very little decrease in the fracture toughness for nano-composite with 10 wt. % of SiC (nm).

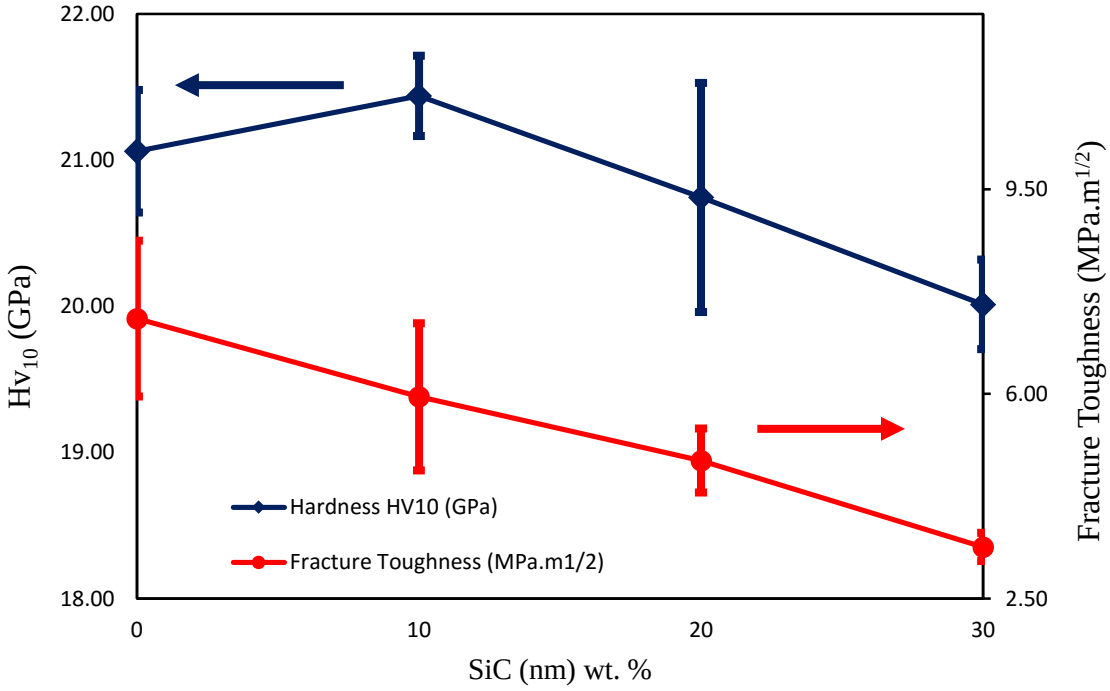

Figure 31: Trend of mechanical properties of SiC (nm)/α-SiAlON nano-composite ceramics

The backscattered electron microscopy images of the fracture surfaces of monolithic α-SiAlON (1530), and SiC(nm)/α-SiAlON nano-composites with 10, 20 and 30 wt. % of SiC (nm) are shown in Figure 32 (a), (b), (c) and (d) respectively. The monolithic α-SiAlON sample (1530) having higher values of fracture toughness exhibited a coarse fracture surface which is associated with toughening mechanism. However, the fracture of the composite samples was quite brittle as there fracture surfaces were relatively smooth and very scarce irregularities were found in the fractographs which is a feature of brittle fracture [56]. The fracture surface of sample 1530-1SiC(nm) seemed to show some ups and downs which probably could explain the relative high fracture toughness value as compared to the sample 1530-3SiC(nm) in which very clear and smooth features represented a typical brittle fracture.

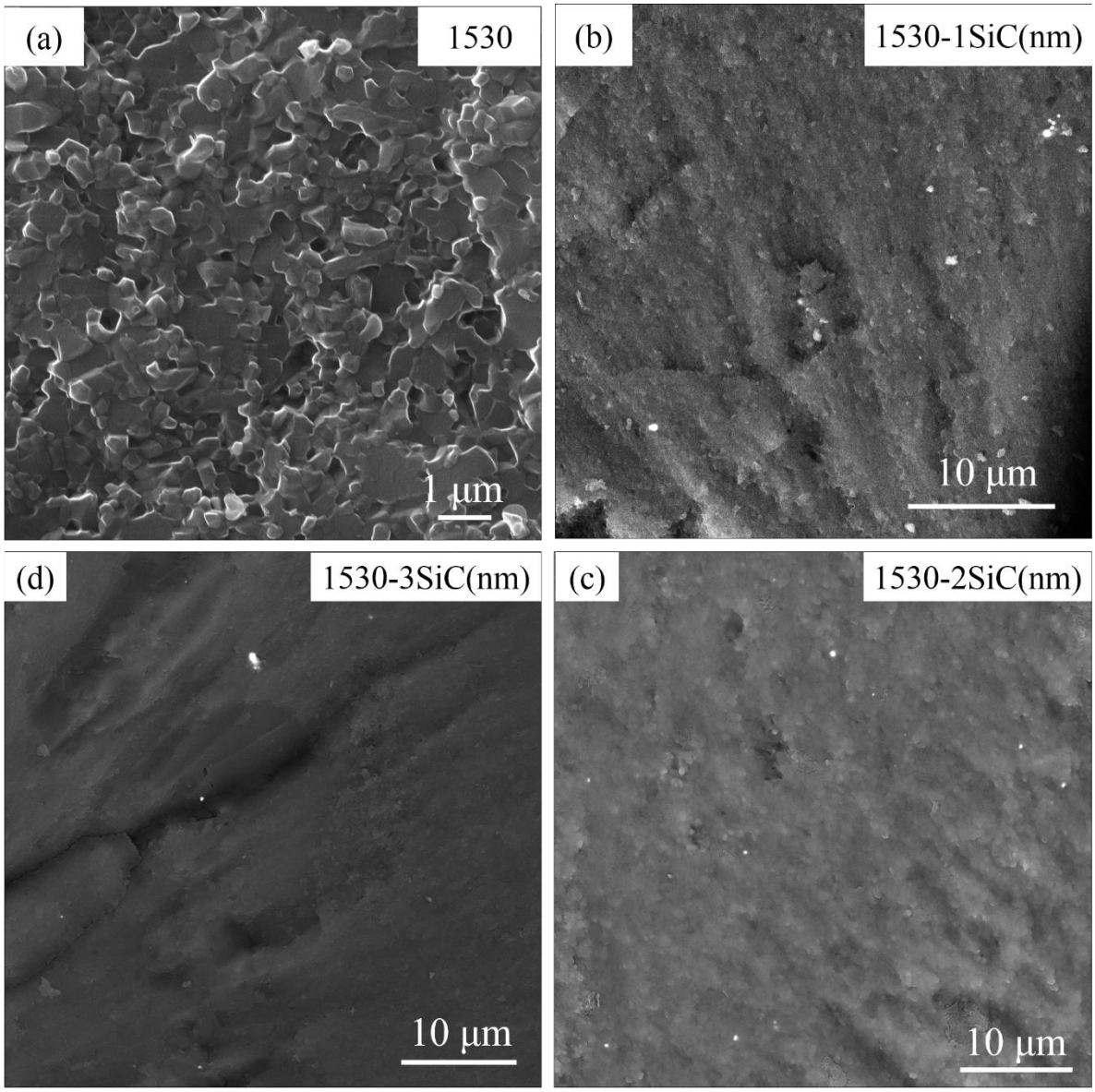

Figure 32: BSE-Fracture surfaces of (a) monolithic α-SiAlON, (b) 10 wt. % (c) 20 wt. % (d) 30 wt. % SiC(nm)/α-SiAlON nano-composites

Figure 33 shows scanning electron micrograph of Vickers indentation introduced in nano-composite ceramic with 20 wt. % of SiC (nm), sample 1530-2SiC(nm). The radial and lateral cracking along with material scalloping from the contact zone of indentation was clearly visible in almost all the indents. Such type of indentation is associated with brittle materials with low fracture toughness. It should also be noted that lateral cracking and material removal did not make the hardness values ambiguous [63, 64].

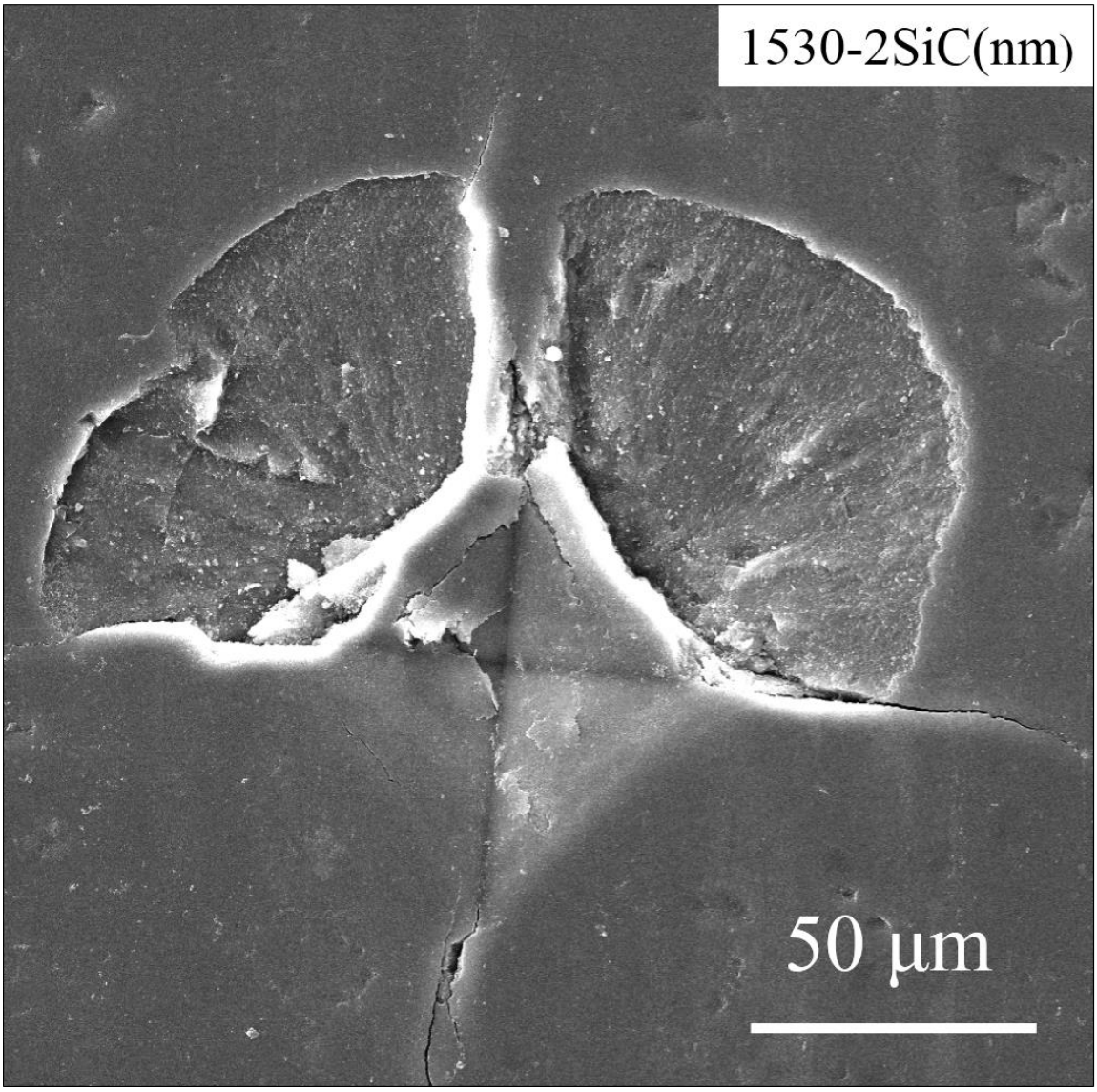

Figure 33: SEM-Vickers indent illustrating lateral cracks in nano-composite ceramic with 20 wt. % of SiC (nm)

4.2.3 Micron Tungsten Carbide-WC (μm)/α-SiAlON Composite

Table 15 shows the sample name and amount of WC (μm) added in each batch of the matrix powder. The sample name depicted the sintering condition and the amount of reinforcement added, for an instance the sample named 1530-1WC(μm) means sample sintered at 1500 °C with 30 min holding time containing 10 wt. % of WC (μm).

Table 15: Wt. % of WC (μm) in each batch of the matrix for the powder composites

Sample Name	Matrix	WC (μm) wt. %
1530-1WC(μm)	α-SiAlON	10
1530-2WC(μm)	α-SiAlON	20
1530-3WC(μm)	α-SiAlON	30

Sintering and Densification

The samples containing 10, 20 and 30 wt. % of WC (μm) were synthesis following the experimental procedure mentioned earlier and, there experimental and calculated densities were determined as shown in Table 16. The theoretical densities were calculated using rule of mixture. It was illustrated from the density data that with 10 wt. % addition of WC (μm) above 99 % densification was achieved but with increase in amount of WC (μm) the percentage densification was found to be decreasing which could be attributed to mixing process setbacks or decrease in level of dispersion of WC (μm) in the matrix.

Table 16: Densification of WC (μm)/α-SiAlON composite ceramics

Sample Name	Experimental Density (g/cm^3)	Theoretical Density (g/cm^3)	Percentage Densification
1530	3.19	--	--
1530-1WC(μm)	3.44	3.47	99.13
1530-2WC(μm)	3.67	3.79	96.83
1530-3WC(μm)	3.89	4.19	92.84

Phase Analysis

Figure 34 show the x-ray phase assemblage for monolithic sample with zero wt. % WC (μm), sample 1530, and composite samples with 10, 20 and 30 wt. % of WC (μm), samples 1530-1WC(μm), 1530-2WC(μm) and 1530-3WC(μm) respectively. As mentioned before sample-1530 illustrated the presence of only α-SiAlON and in composite sample typical behavior of two phase system was prominent i.e. the intensities of the peaks were found to increase with the increase in the amount of WC (μm) particles. Moreover no other peaks were found other than the inculcated WC particles and α-SiAlON matrix which depicted that there was no chemical interaction between the matrix and the second phase WC (μm) particles [26].

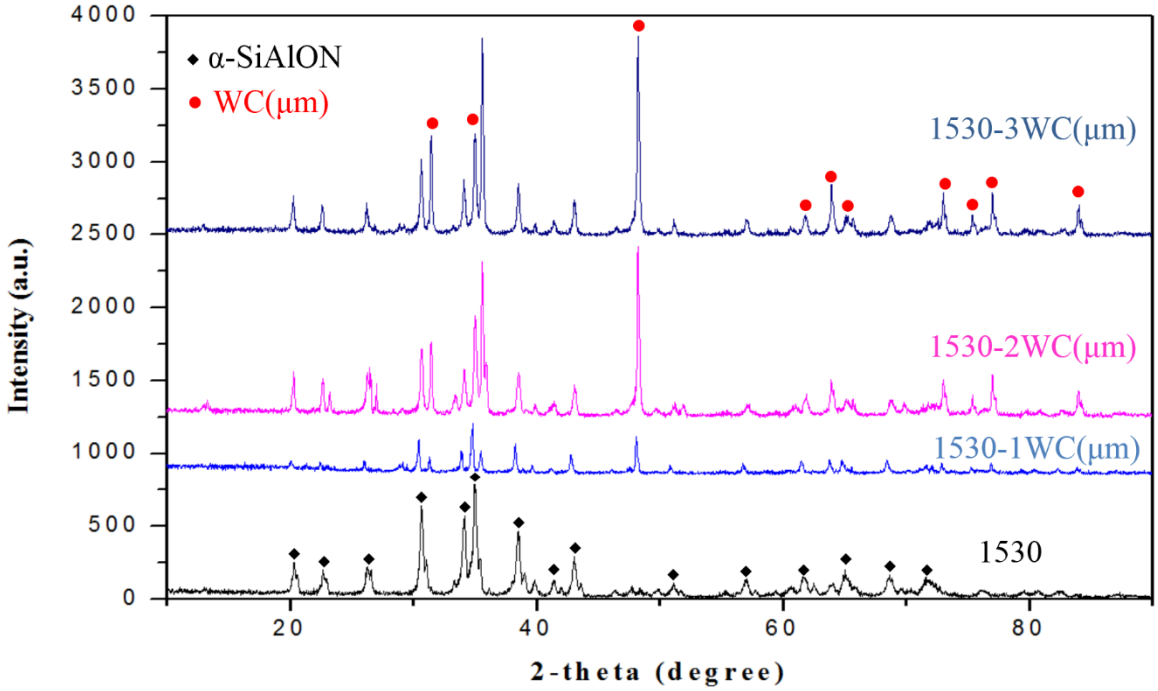

Figure 34: XRD of monolithic α-SiAlON, 10 wt. %, 20 wt. % and 30 wt. % WC(μm)/α-SiAlON composites

Microstructural Analysis

Figure 35 (a), (b) and (c) show back scattered electron micrographs of sample 1530-1WC(μm), 1530-2WC(μm) and 1530-3WC(μm) respectively containing 10, 20 and 30 wt. % of WC (μm) respectively in α-SiAlON matrix along with the EDS-mapping for tungsten showing the dispersion of tungsten carbide in the matrix. The dark area shows the matrix α-SiAlON while bright white particles are tungsten carbide reinforcements. As illustrated in Figure 35 (a), sample with 10 wt. % of WC (μm), there was homogeneous dispersion of particles while in Figure 35 (b) and (c) representing sample with 20 and 30 wt. % WC (μm) respectively, patches of agglomerations of tungsten carbide were found. The decreased in density for these two samples also correlated the inhomogeneity in the dispersion of the second phase. The most probable reason for the decrease in the level of dispersion of WC could be attributed to the drying process of the mixture (powder mixture with ethanol), after probe sonication. The heavy tungsten carbide particles (density =15.6 g/cm^3) could settle down earlier than the rest of precursors to form agglomerations. [53]. Although after drying the mixtures were mixed manually in mortar and pestle to avoid such inhomogeneous dispersion. It should also be noted that composite samples containing SiC (μm) were also processed in similar manner but due to the comparable densities of SiC (3.21 g/cm^3) and Si_3N_4 (3.44 g/cm3) the settling time (during drying) for the mixture could be assumed to be the same.

These agglomerations in the sample containing higher amount of WC (μm), made the mechanical properties data vulnerable to errors. Therefore, in the coming sections, only sample 1530-1WC(μm) with 10 wt. % of WC is considered in detail.

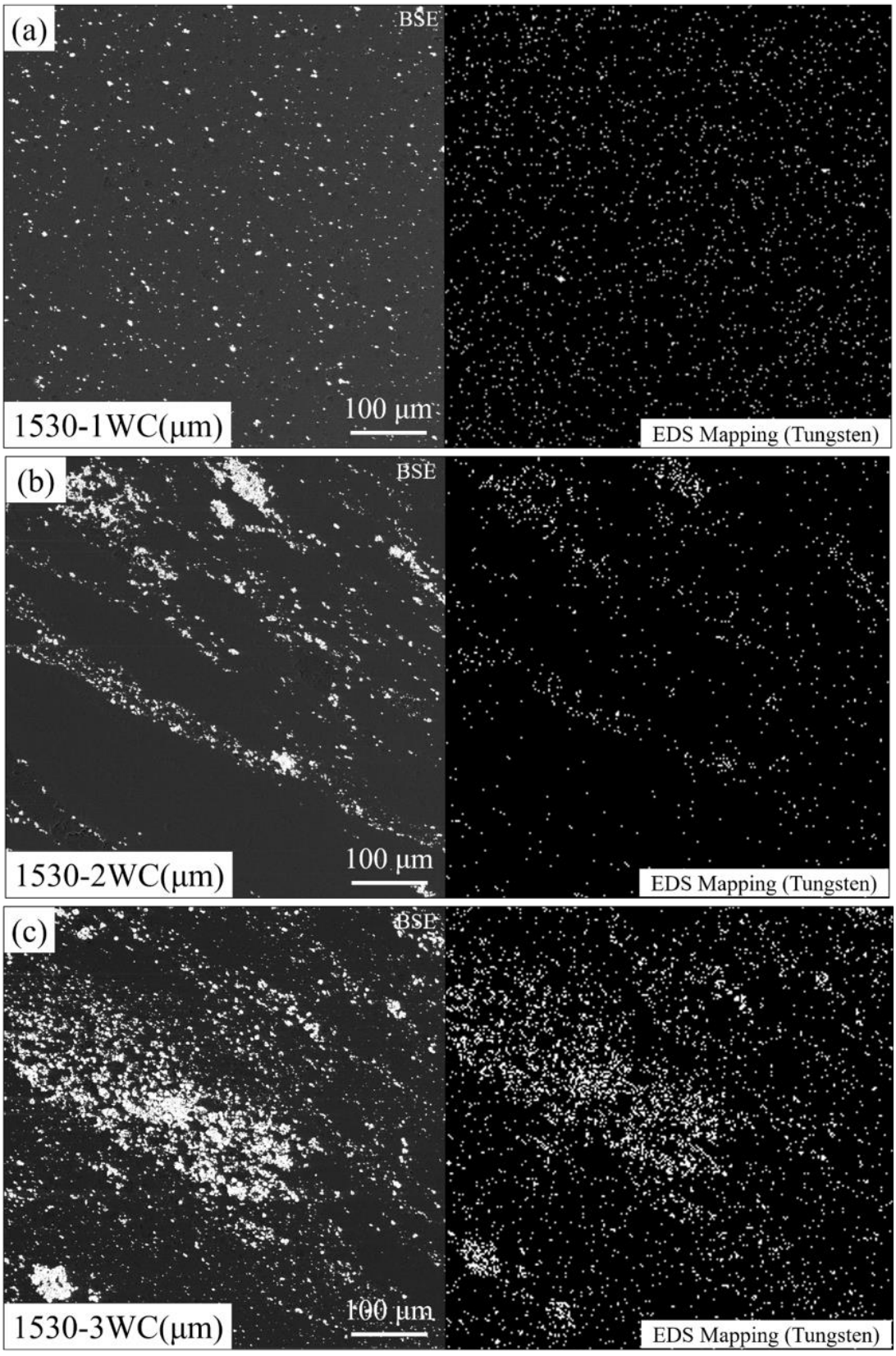

Figure 35: BSE micrographs and EDS mapping of samples with (a) 10 wt. %, (b) 20 wt. % and (c) 30 wt. % of WC (μm) in α-SiAlON matrix

Mechanical Properties

The mechanical properties, hardness and fracture toughness, of the reinforced composite ceramics are shown in Table 17. The sample with 10 wt. % WC (μm), sample 1530-1WC(μm) is showing excellent properties. Especially fracture toughness value showed a tremendous increase from 7.29 MPa.$m^{1/2}$ to 19.42 MPa.$m^{1/2}$, in comparison to the only single literature source found for tungsten carbide inculcation in SiAlON matrix, where fracture toughness value decreased with the addition of tungsten carbide (maximum value being 6.1 MPa.$m^{1/2}$ with 10 vol. % of WC addition in SiAlON matrix possessing fracture toughness of 7 MPa.$m^{1/2}$) [49].

Table 17: Mechanical properties of WC (μm)/α-SiAlON composite ceramics

Sample Name	Hardness HV_{10} (GPa)	Fracture Toughness (MPa.$m^{1/2}$)
1530	21.06 ± 0.42	7.29 ± 1.33
1530-1WC(μm)	23.46 ± 0.29	19.42 ± 0.25
1530-2WC(μm)	21.84 ± 0.77	15.77 ± 4.68
1530-3WC(μm)	22.56 ± 0.44	12.79 ± 3.60

In the present work, the fracture toughness measured for composite ceramics with 20 and 30 wt. % amount of tungsten carbide showed huge error in the readings, see Figure 36, which were considered not reliable. The probable reason for such disturbing trend in the properties could be the mixing procedure used resulting in inhomogeneous dispersion of WC (μm) particles in matrix, as depicted by SEM micrographs. It is well known that in composite ceramics the dispersion of the second phase particle has a huge effect on the density and as a consequence on the mechanical properties [62].

It should also be noted that the fracture toughness (19.42 MPa.$m^{1/2}$) of sample 1530-1WC(μm) was about 1.5 times higher than the fracture toughness (7.29 MPa.$m^{1/2}$) of monolithic α-SiAlON, while the hardness was about 11 percent higher. The homogeneity in dispersion and complete densification of composite ceramics with 10 wt % addition of WC (μm) could be associated to such marvelous properties. The higher hardness of the composite ceramics could be ascribed to the high hardness of the inculcated second phase particles.

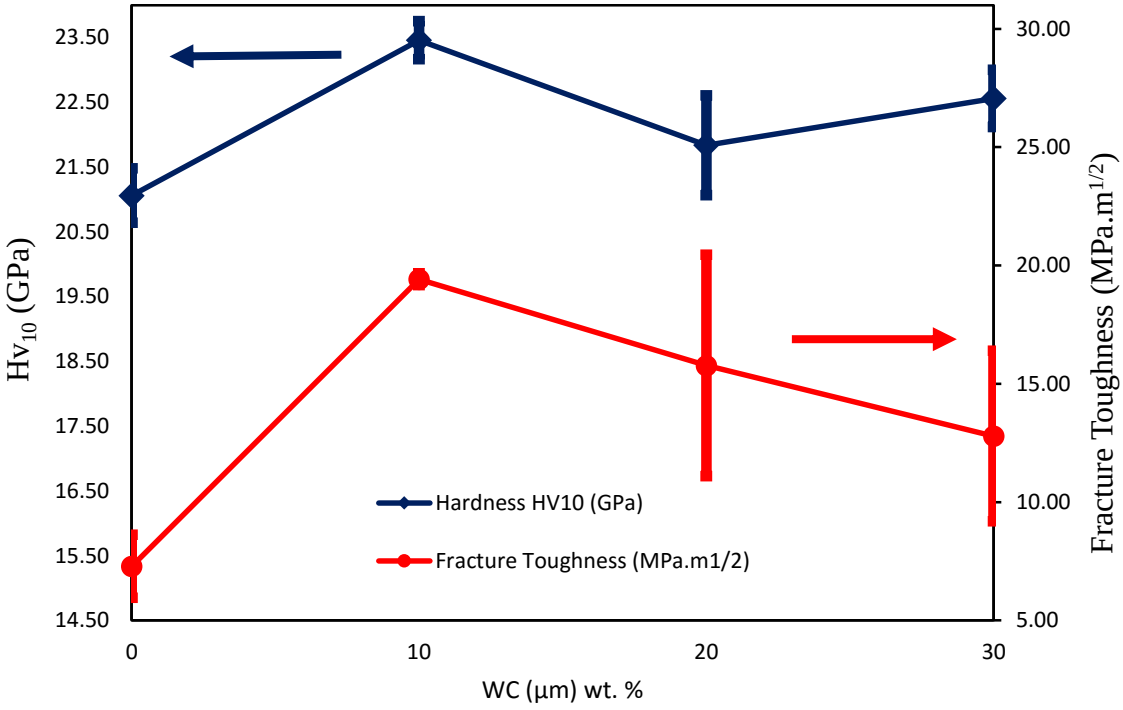

Figure 36: Trend of mechanical properties of WC (µm)/α–SiAlON composite ceramics

Scanning electron microscopy of the fracture surface of monolithic α-SiAlON and sample with 10 wt. % WC (μm) particles are shown in Figure 37 (a) and (b) respectively. The fracture surface of monolithic α-SiAlON, exhibiting relatively lower fracture toughness, as explained before showed a predominant intergranular mode of fracture. While the sample with 10 wt. % of WC (μm), showing very high fracture toughness values, depicted a variety of toughening mechanisms. The addition of hard second phase particles could cause anisotropic growth of α-SiAlON producing elongated grains which introduced toughening in the composite. In addition to this, these elongated grains also induced friction pull outs as depicted by the fracture surface Figure 37 (b). It was also observed that probable cleavage rising present in the fracture surface could have assisted the fracture toughness. Coarse and rough fracture surface along with variety of irregular features on the fracture surface yield a much tougher ceramic [55] [56].

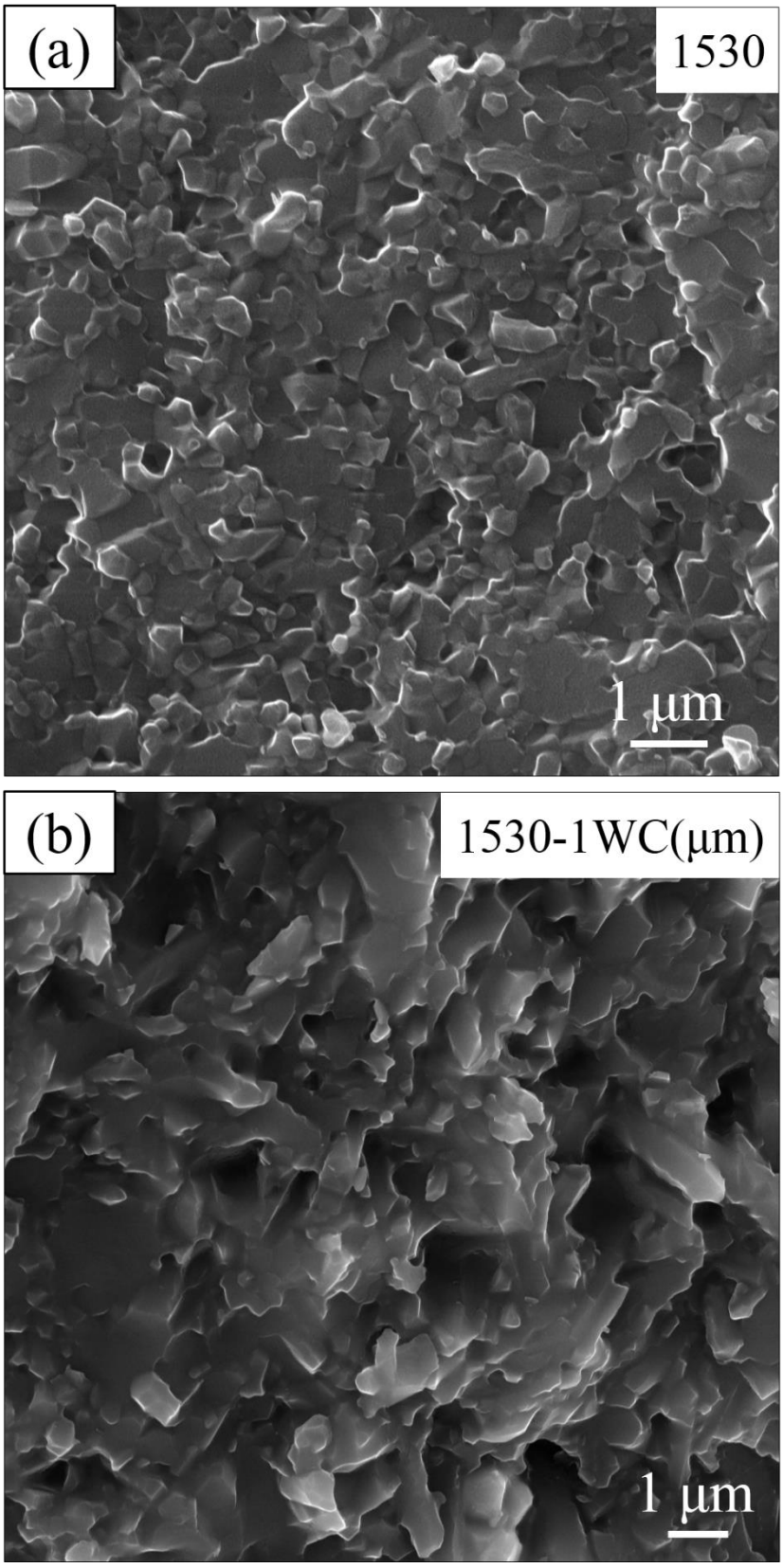

Figure 37: SEM-Fracture surface of (a) Monolithic α-SiAlON and (b) 10 wt. % WC (μm)/α-SiAlON composite

Figure 38 (a, b) and (c, d) show the Vickers indentation along with the crack propagation in monolithic α-SiAlON sample (1530) and sample with 10 wt.% of WC (μm) (1530-1WC(μm)) respectively. It was illustrated from these micrographs that sample 1530 showed a fast crack propagation as the crack was not deflected on its way, Figure 38 (b). While, from the crack propagation in sample 1530-1WC(μm), it was obvious that crack was deflected, Figure 38 (d). Very clear crack bridging phenomenon was also seen in crack propagated in sample 1530-1WC(μm). The fracture toughness of the composite ceramic was considerably increased due to such phenomenon of crack bridging and crack deflection, as significant amount of energy was absorbed at these points before leading to failure [65] [57] [52].

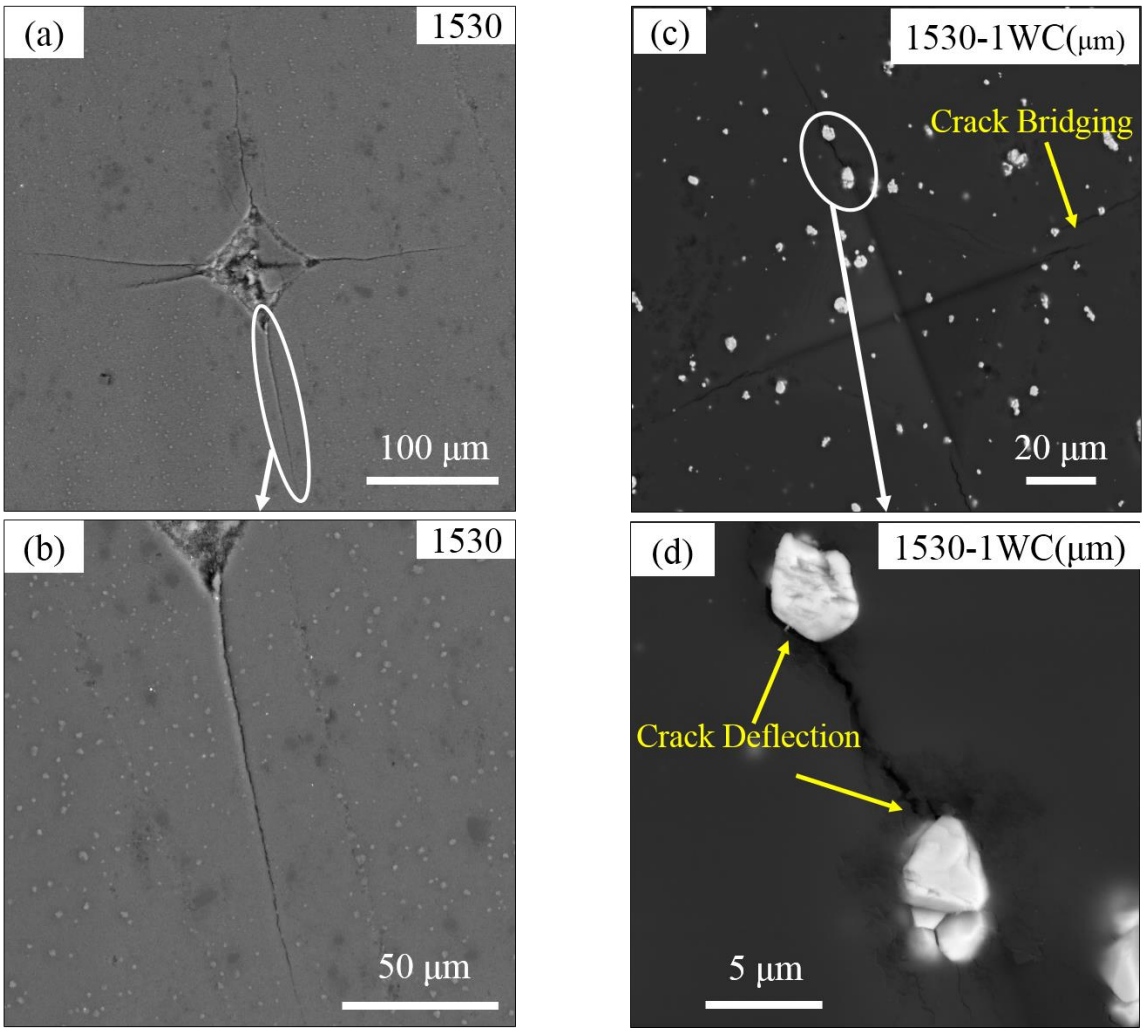

Figure 38: BSE-Comparison of indentation and crack propagation in (a, b) monolithic α-SiAlON and (c, d) 10 wt. % WC (µm)/α-SiAlON composite

CHAPTER 5

CONCLUSIONS AND RECOMMENDATIONS

5.1 Conclusions

Single phase monolithic α-SiAlON ceramics have been fabricated from nano-sized precursors using spark plasma sintering (SPS) technique at temperatures of 1500 °C and 1600 °C with varying holding times from 10 to 30 minutes at an applied pressure of 50 MPa under vacuum. The effects of nano precursors and sintering parameters on the microstructure, densification and mechanical properties were investigated. The following conclusions were drawn from synthesis of monolithic ceramics:

- Monolithic single phase α-SiAlON was produced using nano-sized starting powders and SPS at 1500 °C for 30 min dwell time, yielding hardness and fracture toughness values of 21.05 GPa (Hv_{10}) and 7.29 MPa.$m^{1/2}$ respectively.
- When α-SiAlON was sintered at 1600 °C for 30 min holding time, the hardness and fracture toughness were measured to be 20.50 GPa (Hv_{10}) and 9.65 MPa.$m^{1/2}$ respectively. The increase in fracture toughness compared to α-SiAlON sintered at 1500 °C was attributed to the elongation of the α-SiAlON grains.

The α-SiAlON sintered at 1500 °C was selected as a matrix for preparing the composites using silicon carbide (SiC) and tungsten carbide (WC) reinforcements (10 20 & 30 wt. %), and the following conclusions were drawn:

- The dispersion of second phase particles in the consolidated composite ceramics with SiC (~ 2 μm) reinforcement (10 20 & 30 wt. %) was found to be homogeneous. Composite ceramic with WC (3.5 μm) reinforcement showed a homogenous dispersion for composite with 10 wt. % WC, but poor distribution with higher percentages (20 & 30 wt. %). For the nano-composite α-SiAlON ceramics with nano-sized silicon carbide SiC (50 nm), the reinforcement (10 20 & 30 wt. %) was not homogeneously distributed in the matrix but rather formed clusters.
- For α-SiAlON composites reinforced with SiC (μm), the highest hardness of 24.53 GPa (Hv_{10}) and highest fracture toughness of 11.86 MPa.$m^{1/2}$ were achieved for 30 wt. % of SiC (μm).
- For α-SiAlON/10 wt. % WC (μm) composite, the hardness and fracture toughness were measured to be 23.46 GPa (Hv_{10}) and 19.42 MPa.$m^{1/2}$ respectively.

5.2 Recommendations

Based on the work carried out in this study, the following recommendations are proposed for future work:

- More in-depth analysis of mixing the starting powders should be made to prepare more homogeneously distributed α-SiAlON composites reinforced with nano-SiC as well as high loading of WC (3.5 μm).

- Testing the wear behavior of the sintered SiAlON samples, both at ambient and elevated temperatures, to simulate their application as cutting tools.

References

[1] F. L. F. L. Riley, "Silicon Nitride and Related Materials," *Journal of the American Ceramic Society,* vol. 83, no. 2, pp. 245-265, 2000.

[2] H. S., "The Role of Additives in the Pressureless Sintering of Nitrogen Ceramics for Engine Applications," *Metals Forum,* vol. 7, pp. 162-170, 1984.

[3] H. S., "Silicon Nitride Ceramics," *Materials Science Forum,* 2009.

[4] H. P. D. T. a. K. J. Hampshire S., " α′-Sialon Ceramics," *Nature,* pp. 880-882, 1978.

[5] Y. a. O. K. Oyama, "Solid Solubility of Some Oxides in Si_3N_4," *Japanese Journal of Applied Physics,* vol. 10, no. 11, 1971.

[6] a. W. W. Jack. KH, "Ceramics Based on the Si-Al-ON and Related Systems," *Nature,* vol. 238, no. 80, pp. 28-29, 1972.

[7] L. G. J. B. a. F. A. Izhevskiy VA, "Progress in Sialon Ceramics," *Journal of the European Ceramic Society,* vol. 20, no. 13, pp. 2275-2295, 2000.

[8] E. T. a. M. Nygren., "Siaion Ceramics," *Journal of the American Ceramic Society,* vol. 75, 1992.

[9] H. Mandal, " New Developments in α-Sialon Ceramics." 19.13 (1999): 2349-57.," *Journal of the European Ceramic Society,* vol. 19, no. 13, pp. 2349-2357, 1999.

[10] I. S. a. D. J. Kim, "Growth of Elongated Grains in α-Sialon Ceramics," *Materials Letters,* vol. 47, no. 6, pp. 329-333, 2001.

[11] I.-W. C. a. A. Rosenflanz, "A Tough Sialon Ceramic Based on α- Si_3N_4 with a Whisker-like Microstructure," *Nature,* vol. 389, no. 6652, pp. 701-704, 1997.

[12] Y. Cai, "Synthesis and Characterization of Nitogen-rich Calcium α-Sialon Ceramics," 2009.

[13] M. S. H. a. A. B. Herrmann, "Kinetics of Rare Earth Incorporation and Its Role in Densification and Microstructure Formation of α-Sialon," *Journal of the European Ceramic Society,* vol. 32, no. 7, pp. 1313-1319, 2012.

[14] Y. V. P.-B. a. S. H. Menke, "Effect of Rare-Earth Cations on Properties of Sialon Glasses," *Journal of non-crystalline solids* , vol. 276, no. 1, pp. 145-150, 2000.

[15] S. M. H. a. G. P. Bandyopadhyay, "Effect of Different Rare Earth Cations on the Densification Behaviour of Oxygen Rich A-Sialon Composition," *Ceramics international* , vol. 25, no. 3, pp. 207-213, 1999.

[16] G. R. M. a. G. Z. Cao, " Relations between Composition and Microstructure of Sialons," *Journal of the European Ceramic Society,* vol. 11, no. 2, pp. 115-122, 1993.

[17] P. C. Z. W. S. a. D. Y. Wang, "Formation Behavior of Multi-Cation α-Sialons Containing Calcium and Magnesium," *Materials Letters,* vol. 38, no. 3, pp. 178-185, 1999.

[18] P. Y. L. a. D. Y. Wang, "Effect of Dual Elements (Ca, Mg) and (Ca, La) on Cell Dimensions of Multi-Cation α-Sialons," *Journal of the European Ceramic Society* , vol. 20, no. 9, pp. 1333-1337, 2000.

[19] J. H. H. a. R. M. Van Rutten, "Densification Behaviour of Ca-α-Sialons," *Ceramics international*, vol. 27, no. 4, pp. 461-466, 2001.

[20] T. E. a. P.-O. Olsson, "β-Sialon Ceramics with TiN Particle Inclusions," *Journal of the European Ceramic Society,* vol. 13, pp. 551-559, 1994.

[21] Z. H. H. Z. L. L. Y. Z. Feng Ye, "Spark plasma sintering of cBN/β-SiAlON composites," *Materials Science and Engineering A*, vol. 527, pp. 4723-4726, 2010.

[22] D. T. A. B. Z.B. Yu, "Fabriction and characterisation of SiC fibre reinforced Lithium-α-SiAlON matrix composites," *Composites*, vol. Part A, no. 33, pp. 621-629, February 2002.

[23] A. K. Erhan Ayas, "Novel electrically conductive α-β SiAlON/TiCN composites," *Journal of the European Ceramic Society,* vol. 31, pp. 903-911, 2011.

[24] M. J. G.-J. P. M. a. M. O. Belmonte, "Spark Plasma Sintering: A Powerful Tool to Develop New Silicon Nitride-Based Materials," *Journal of the European Ceramic Society* , vol. 30, no. 14, pp. 2937-2946, 2010.

[25] D. Z. S. a. P. Š. Salamon, "Rapid Formation of α-Sialon During Spark Plasma Sintering: Its Origin and Implications," *Journal of the European Ceramic Society* , vol. 27, no. 6, pp. 2541-2547, 2007.

[26] F. Y. Z. Z. a. Y. Z. Limeng Liu, "Elongation of α-SiC particles in spark plasma sintered α-SiAlON/α-SiC composites," vol. 94, pp. 336-339, 2011.

[27] C. O. &. R. P. J. Sjoberg, "The Effect of Yttria Additions on the Composition of O'-Sialons Prepared by Pressureless Sintering," *Journal of the European Ceramic Society,* vol. 10, pp. 41-50, 1992.

[28] D. J. S. T. J. G. Shaoming Dong, "Hot isostatic pressing and post-hot isostatic pressing of SiC-β-SiAlON composites," *Materials Letters,* no. 29, pp. 259-263, June 1996.

[29] W. Z. T. A. Xuemei Yi, "Thermal conductivity of β-SiAlONs prepared by a combination of combustion synthesis and spark plasma sintering," *Thermochimica Acta,* vol. 576, pp. 56-59, 2014.

[30] A. K. H. M. S. T. F. K. Erhan Ayas, "Decolouration effect of WC addition on gas pressure sintered α-β SiAlON Ceramics," *Materials Letter,* vol. 58, pp. 1498-1501, 2004.

[31] Y.-B. C. B. C. M. L. G. T. S. Y. H. Wang, "Microstructure and mechanical mechanical properties nanoscale SiC/Ca α-SiAlON composites," *Journal of Materials Science,* vol. 32, pp. 3263-3269, 1997.

[32] D. P. T. &. H. M. Necip Camuscu, "Effect of Starting Composition, Type of Rare Earth Sintering Additive and Amount of Liquid Phase on α-β Sialon Transformation," *Journal of the European Ceramic Society,* vol. 17, pp. 599-613, 1997.

[33] E. N. K. K. J. T. T. M. C. Zhang, "Control of grain morphology in Ca-α-sialon ceramics by changing the heating rate," *Materials Letters,* vol. 43, pp. 315-319, May 2000.

[34] M. J. H. S. H. M. I. Feng Ye, "Microstructural development of Y-α/(β)-sialons after post heat-treatment and its effect on mechanical properties," *Ceramics International,* vol. 30, pp. 229-218, 2004.

[35] H. H. R. M. J.W.T. van Rutten, "Densification behavior of Ca-alpha-sialons," *Ceramics International,* vol. 27, pp. 461-466, 2001.

[36] O. D. Nurcan Calis Acikbasn, "The effect of cation type, intergranular phase amount and cation mole ratios on z value and intergranular phase crystallization of SiAlON ceramics," *Ceramics International,* vol. 39, pp. 3249-3259, 2013.

[37] I. S. ,. M. H. S. Kurama, "Wear properties of α- and α/β-SiAlON ceramics obtained by gas pressure sintering and spark plasma sintering," *Journal of the European Ceramic Society,* vol. 31, pp. 921-930, 2011.

[38] Y. Akimune, "High-temperature strength of SiC whisker-SiAlON composites," *Journal of Materials Science Letters,* pp. 816-817, 1990.

[39] N. H. T. O. Yoshio Akimune, "Mechanical properties of SiC-particle SiAlON composites," *Journal od Materials Science Letters 10,* pp. 223-226, 1991.

[40] Y. X. D. Z. a. W. M. K. Chao M. Huang, "Combustion-Synthesized β-SiAlON Reinforcement with SiC Monofilaments," *Materials Science and Engineering,* pp. 341-351, February 1994.

[41] D. Z. Y. X. W. M. K. C. Y. Y. Chao M. Huang, "SiC_f/O-SiAlON composite: properties and oxidation retained properties," *Materials Science and Engineering,* pp. 176-184, June 1996.

[42] P. Palmero, "Structural Ceramic Nanocomposites: A Review of Properties and Powders' Synthesis Methods," *nanomaterials*, no. 5, pp. 656-696, 2015.

[43] K. U. T. Inoue, "Preparation and properties of SiC fibre reinforced SiAlON ceramic composite," *Ceramics International,* vol. 23, pp. 165-170, 1997.

[44] L. G. D. J. C. Z. D. Y. Qiang Li, "Preparation of β-SiAlON/nano-SiC composites," *Journal of Materials Science Letters,* vol. 16, pp. 1620-1621, 1997.

[45] L. G. D. Y. D. T. Q. Liu, "Hard SiAlON cceramics reinforced with SiC nanoparticles," *Materials Science and Engineering,* vol. A269, pp. 1-7, 1999.

[46] C. A. S. R. K. S. J. S. O. S. C. Santos, "α-SiAlON-SiC composites obtained by gas-pressure sintering and hot-pressing," *Journal of Materials Processing Technology*, vol. 189, pp. 138-142, January 2007.

[47] C. S. C. K. O. S. J.V.C. Souza, "Development of α-SiAlON-SiC ceramic composites by liquid phase sintering," *International Journal of Refractory Metals & Hard Materials*, vol. 25, pp. 77-81, 2007.

[48] F. Y. Y. Z. Limeng Liu, "Microstructure and mechanical properties of the α-SiAlON/α-SiC composites: Effects of heat treatment," *Ceramics International*, vol. 37, pp. 3737-3741, May 2011.

[49] S. B. K. F. Bernd Bitterlich, "SiAlON based ceramic cutting tools," *Journal of the Europen Ceramic Society*, vol. 28, pp. 989-994, 2008.

[50] K. H. Jack, "Review: Sialons and related nitrogen ceramics," *Journal of Materials Science*, pp. 1135-1158, 1976.

[51] Y. D. C. M. A. a. L. L. Torres, "Fracture Toughness Evaluation of Hardmetals: Influence of Testing Procedure.," *International Journal of Refractory Metals and Hard Materials*, vol. 19, no. 1, pp. 27-34, 2001.

[52] L. L. H. Z. Y. Z. a. Z. Z. Feng Ye, "Novel mixed α/β-SiAlONs with both elongated α and β grains," *Scripta Materialia*, no. 60, pp. 471-474, 2009.

[53] M. Sternitzke, "Review: Structural Ceramic Nanocomposites," *Journal of the European Ceramic Society*, no. 17, pp. 1061-1082, 1997.

[54] H. Yurdakul, "Microstructural investigation of α-β SiAlON/SiC composites by analytical transmission electron microscopy," *Journal of the ceramic society of Japan,* vol. 3, no. 123, pp. 136-141, 2015.

[55] H. Y. X. Z. a. L. Z. Xingzhong Guo, "Preparation and properties of nano-SiC-based ceramic composites containing nano-TiN," *Scripta Materialia,* no. 68, pp. 281-284, 2013.

[56] R. H. D. a. R. O. R. C. J. Gilbert, "Microstructural Mechanism of Cyclic Fatigue-Crack Propagation in Grain-Bridging Ceramics," *Ceramics International,* no. 23, pp. 413-418, 1997.

[57] Z. Y. V. K. C.R. Zhou, "Pressureless sintered self-reinforced Y-α-SiAlON ceramics," *Journal of the European Ceramic Society,* no. 27, pp. 437-443, 2007.

[58] J. W. Hutchinson, "Mechanisms of Toughening in Ceramics," *Theoretical and Applied Mechanics,* pp. 139-144, 1989.

[59] D. C. M. W. B. T. E.-R. R. O. R. K. Shirato, "High-temperature cyclic fatigue-crack growth in monolithic Ti_3SiC_2 ceramics," *Fatigue and fracture of High temperature materials,* 2000.

[60] J. V. T. L. &. O. V. d. B. Y. Zhou, "Toughening of X-Sialon with Al_2O_3 Platelets," *Journal of the european ceramics society,* no. 15, pp. 297-305, 1995.

[61] F. W. M. E. B. A. I. K. I. Tanguy Rouxel, "Intergranular crack defelection and crystallographic slip in Si_3N_4-SiC nano-composites," *Journal of the European Ceramic Society,* no. 11, pp. 431-438, 1993.

[62] J. Z. &. M. P. H. Laura C. Stearns, "Processing and Microstructure Development in Al_2O_3-SiC 'Nanocomposites'," *Journal q[" the European Ceramic Society,* no. 10, pp. 473-477, 1997.

[63] J. W. H. a. A. G. E. Xi Chen, "The Mechanics of Indentation Induced Lateral Cracking," *J. Am. Ceram. Soc.,* vol. 5, no. 88, pp. 1233-1238, 2005.

[64] R. F. COOK, "Strength and sharp contact fracture of silicon," *J MATER SCI,* no. 41, pp. 841-872, 2006.

[65] J. Z. Y. Z. Z. G. X. C. A. L. G.M. Zheng, "Fabrication and characterization of Sialon–Si_3N_4 graded nano-composite ceramic tool materials," *Composites,* vol. B, no. 42, pp. 1813-1820, 2011.

Vitae

Name	: Raja Muhammad Awais Khan
Nationality	: Pakistani
Date of Birth	: 03-09-1989
Email	: rajaawais89@gmail.com
Address	: Abbottabad, Pakistan
Academic Background	: **Master of Science in Mechanical Engineering, December, 2015**
	Thesis: Effect of Silicon Carbide (SiC) and Tungsten Carbide (WC) Reinforcements on the Properties of α-SiAlON Ceramic-Based Nano Composites
	King Fahad University of Petroleum & Minerals, KSA
	: **Bachelor of Engineering, Mechanical Engineering, January, 2013**
	Final Year Project: Mechanical Characterization (Fatigue Life Prediction) of Honeycomb Sandwich Panels' Material.
	National University of Sciences & Technology (NUST), Pakistan

Publications

1. Abbas Saeed Hakeem, Raja Muhammad Awais Khan, Moath Mohammad Al-Malki, Faheemuddin Patel, Akolade Idris Bakare, Sadaqat Ali, Stuart Hampshire, Tahar Laoui "Development and Processing of SiAlON nano-ceramics by Spark Plasma Sintering", Advances in Science and Technology, Vol. 89, 63-69, 2014

2. Moath Mohammad Al Malki, Raja Muhammad Awais Khan, Abbas Saeed Hakeem, Stuart Hampshire, Tahar Laoui, "Effect of metallic Al precursors on the sinterability and the mechanical properties of SiAlON nano-ceramic prepared by spark plasma sintering." Journal of the European Ceramic Society (submitted)

3. Raja Muhammad Awais Khan, Moath Mohammad Al Malki, Abbas Hakeem, Stuart Hampshire, Tahar Laoui. "Synthesis of single phase Ca-α-SiAlON using nano sized precursors in spark plasma sintering at lower temperatures." Journal of the European Ceramic Society (Under preparation)

4. Moath Mohammad Al Malki, Raja Muhammad Awais Khan, Abbas Saeed Hakeem, Stuart Hampshire, Tahar Laoui, Muhammad Ali Ehsan . “The role of post-sintering heat treatment on the fracture toughness of Ca-α-SiAlON ceramics”. Journal of the European Ceramic Society (Ready for submission)

5. Raja Muhammad Awais Khan, Moath Mohammad Al Malki, Abbas Saeed Hakeem, Stuart Hampshire, Tahar Laoui. "Effect of SiC reinforcement on the wear and mechanical properties of Ca-α-SiAlON ceramics." Journal of the European Ceramic Society (Under preparation)